



저작자표시-비영리-변경금지 2.0 대한민국

이용자는 아래의 조건을 따르는 경우에 한하여 자유롭게

- 이 저작물을 복제, 배포, 전송, 전시, 공연 및 방송할 수 있습니다.

다음과 같은 조건을 따라야 합니다:



저작자표시. 귀하는 원 저작자를 표시하여야 합니다.



비영리. 귀하는 이 저작물을 영리 목적으로 이용할 수 없습니다.



변경금지. 귀하는 이 저작물을 개작, 변형 또는 가공할 수 없습니다.

- 귀하는, 이 저작물의 재이용이나 배포의 경우, 이 저작물에 적용된 이용허락조건을 명확하게 나타내어야 합니다.
- 저작권자로부터 별도의 허가를 받으면 이러한 조건들은 적용되지 않습니다.

저작권법에 따른 이용자의 권리와 책임은 위의 내용에 의하여 영향을 받지 않습니다.

이것은 [이용허락규약\(Legal Code\)](#)을 이해하기 쉽게 요약한 것입니다.

[Disclaimer](#)



이학박사학위논문

콩의 뿌리혹 발달과 애기장대의 제미니바이러스
감염에 미치는 리모린의 영향

Effects of Remorins on Root-nodule Development in
Soybean and Geminivirus Infection in *Arabidopsis*

2014년 8월

서울대학교 대학원

생명과학부

손승민

GENERAL ABSTRACT

Effects of Remorins on Root-nodule Development in
Soybean and Geminivirus Infection in *Arabidopsis*

Seungmin Son

School of Biological Sciences

Seoul National University

Remorin, a plant-specific protein containing variable N-terminal region and conserved C-terminal domain, is known to be involved in various biotic and abiotic stress-response mechanisms, elicited by external stimuli such as host-microbe interactions. However, the roles of remorins in soybean and *Arabidopsis* have not been fully characterized. Thus, to elucidate their functions, I have focused on the role of *GmREM1.1/2.1* and *AtREM4s* in this study.

As mentioned in chapter I, the C-terminal anchor (CA) is essential for the plasma membrane (PM) targeting of *GmREM1.1/1.3*, whereas the CA of

GmREM2.1 does not localize to the PM. *Yeast two-hybrid* (Y2H) and bimolecular fluorescence complementation (BiFC) assays have shown that remorins are involved in homo- and hetero-oligomeric interaction at the PM. However, they do not seem to interact with GmREM2.1. The difference between *GmREM1.1* and *GmREM2.1* was elucidated using a genetic approach. The *GmREM1.1* promoter is active in the inner cortex of root nodules, whereas the *GmREM2.1* promoter is activated in the infected cells. Moreover, unlike the rRNA interference (RNAi) of *GmREM1.1*, the (RNAi) of *GmREM2.1* decreases the extent of nodulation on transgenic roots. These results indicate that GmREM1.1 and GmREM2.1 have distinct molecular characterizations and functions during nodule development.

As describe in chapter II, *AtREM4.1* and *AtREM4.2* had typical characteristics of the remorin molecules, and their expression was dramatically induced by osmotic stress, abscisic acid (ABA), and senescence. During geminivirus infection, the mutant lines of *AtREM4s* showed a reduced susceptibility, whereas the overexpression lines showed the opposite. In addition, they were both regulated by SnRK1 and by the 26S proteasome. Moreover, the co-expression of AtREM4.1 with transcription factor AtTCP14 led to a BiFC signal in the nucleus. These results suggest that AtREM4s could

be involved in a SnRK1-mediated signaling pathway, and that they could play an important role as the positive regulators of cell cycle during geminivirus infections.

Keywords : AtREM, geminivirus, GmREM, root nodule, SnRK1

Student Number : 2010-30098

CONTENTS

GENERAL ABSTRACT	i
CONTENTS	iv
LIST OF TABLES	ix
LIST OF FIGURES	x
ABBREVIATIONS	xii
1. GENERAL INTRODUCTION	1
1.1 Remorin	2
1.1.1 Discovery and annotation of remorin.....	2
1.1.2 Molecular and functional characterization of remorin.....	2
1.1.3 Six groups of remorin family.....	5
1.1.4 Intrinsically disordered N-terminal region.....	6
1.1.5 The conserved C-terminal domain in remorin.....	8
1.2 Plasma membrane partitioning	12
1.2.1 Plasma membrane.....	12
1.2.2 Microdomain of plasma membrane.....	12

1.2.3 Microdomain-associated proteins.....	14
1.3 Scaffold protein.....	15
1.3.1 Definition of scaffold.....	15
1.3.2 Function of scaffold protein.....	15
1.3.3 Homer scaffold protein.....	17
1.4 Purpose of the study.....	19
2. CHAPTER I. GmREM1.1 and GmREM2.1, which encode the remorin proteins in soybean, have distinct roles during root nodule development.....	20
2.1 Abstract.....	21
2.2 Introduction.....	22
2.3 Materials and methods.....	25
2.3.1 Plant materials and bacterial strains.....	25
2.3.2 Plasmid construction.....	25
2.3.3 Yeast two-hybrid assay.....	26
2.3.4 Bimolecular fluorescence complementation (BiFC) and localization of GFP-conjugated proteins.....	27
2.3.5 Generation of transgenic hairy roots and nodules.....	28

2.3.3 Histochemical GUS analysis.....	29
2.4 Results.....	32
2.4.1 Intra- and intergenic protein-protein interactions of GmREMs	
.....	32
2.4.2 A short C-terminal anchor targets GmREM1.1 and GmREM1.3	
to the PM.....	36
2.4.3 <i>GmREM1.1</i> and <i>GmREM2.1</i> have distinct spatial expression	
patterns in root nodules.....	39
2.4.4 Silencing of <i>GmREM2.1</i> leads to decreased nodule formation	
.....	41
2.5 Discussion.....	44

3. CHAPTER II. <i>Arabidopsis thaliana</i> remorins interact with	
SnRK1 and play a role in susceptibility to beet curly top and	
beet severe curly top viruses.....	50
3.1 Abstract.....	51
3.2 Introduction.....	53
3.3 Materials and methods.....	58
3.3.1 Plant materials and virus inoculation.....	58

3.3.2 Sequence analyses.....	59
3.3.3 Gene expression analysis.....	59
3.3.4 Yeast two-hybrid assay.....	60
3.3.5 Bimolecular fluorescence complementation (BiFC) and localization of fluorescent conjugated proteins.....	61
3.3.6 Expression and purification of recombinant proteins.....	61
3.3.7 <i>In vitro</i> kinase assay.....	62
3.3.8 Cell free degradation assay.....	62
3.4 Results.....	67
3.4.1 Transcription of <i>AtREM4s</i> is highly enhanced by osmotic stress, abscisic acid and senescence.....	67
3.4.2 AtREM4 proteins form homo- and hetero-interactions in the plasma membrane.....	71
3.4.3 Double mutants of <i>AtREM4s</i> reduce the BCTV and BSCTV susceptibility.....	75
3.4.4 AtREM4s interact with SnRK1.2 and AtREM4.1 is phosphorylated by it.....	79
3.4.5 AtREM4s are degraded by the 26S proteasome pathway.....	83
3.4.6 Protein interactions leading to subcellular AtREM4.1	

redistribution.....	86
3.5 Discussion.....	90
REFERENCES.....	97
ABSTRACT IN KOREA.....	115

LIST OF TABLES

CHAPTER I.

Table 2. Primers used for constructs.....	30
---	----

CHAPTER II.

Table 3-1. Primers used for RT-PCR.....	64
---	----

Table 3-2. Primers used for constructs.....	65
---	----

LIST OF FIGURES

GENERAL INTRODUCTION

Figure 1. Six groups and protein domains of the remorin family 11

CHAPTER I.

Figure 2-1. Determination of essential domains for GmREM1.1 dimerization
and physical interactions between GmREM1.1/1.3/2.1 34

Figure 2-2. The plasma membrane targeting of GmREM1.1/1.3/2.1 37

Figure 2-3. Promoter analysis of *GmREM1.1/2.1* 40

Figure 2-4. The total nodule numbers of *GmREM*-silenced transgenic
roots 42

CHAPTER II.

Figure 3-1. Amino acid alignment and expression level of *AtREM4s* 69

Figure 3-2. Subcellular localization and oligomeric interactions of
AtREM4s 73

Figure 3-3. Geminivirus susceptibility of *AtREM4s* 77

Figure 3-4. Phosphorylation of AtREM4s by SnRK1.2 <i>in vitro</i>	81
Figure 3-5. Cell free degradation of recombinant AtREM4 proteins.....	84
Figure 3-6. AtRME4.1 protein-protein interactions and cellular translocations <i>in planta</i>	88
Figure 3-7. Proposed model for how AtREM4s may regulate cell cycle progression during geminivirus infection.....	95

ABBREVIATIONS

3'	three prime end of DNA fragment
35S	35S promoter of cauliflower mosaic virus
5'	five prime end of DNA fragment
a.a.	amino acid
ABA	abscisic acid
ATP	adenosine triphosphate
BiFC	bimolecular fluorescence complementation
bp	base pair
BRCT	BRCA1 C-terminus
RemCA	remorin C-terminal anchor
cDNA	complementary deoxyribonucleic acid
CFP	cyan fluorescent protein
DAI	day after inoculation
DNA	deoxyribonucleic acid
DTT	dithiothreitol
<i>E. coli</i>	<i>Escherichia coli</i>

EDTA	ethylene diamine tetra acetic acid
FHA	forkhead-associated
GFP	green fluorescent protein
GUS	β -glucuronidase
h	hour
kDa	kilodalton
min	minute
MS	Murashige-Skoog
PAGE	polyacrylamide gel electrophoresis
PCR	polymerase chain reaction
PM	plasma membrane
PMSF	phenylmethylsulfonyl fluoride
RFP	red fluorescent protein
RNA	ribonucleic acid
RNAi	rRNA interference
RT	reverse transcription
SA	salicylic acid
SDS	sodium dodecyl sulfate
Tris-HCl	2-amino-e-hydroxymethyl-1,3-propanediol and HCl

X-Gluc	5-bromo-4-chloro-3-indolyl-β-D-glucuronide
Y2H	<i>yeast two-hybrid</i>
YEM	yeast extract and mannitol
YFP	yellow fluorescent protein
WAI	week after inoculation

GENERAL INTRODUCTION

1.1 Remorin

1.1.1 Discovery and annotation of remorin

Remorin was screened from the tomato and potato plasma membrane (PM) proteins phosphorylated in the presence of polygalacturonide (Farmer et al., 1989). The previously identified potato PM protein, pp34, along with another homologous protein, were found to be phosphorylated by the oligogalacturonide present in tomatoes (Jacinto et al., 1993). Remorin possesses a hydrophilic profile and is able to attach to the PM. This mode of attachment is analogous to the attachment of remora fish to the bottom of larger fish, hence the name “Remorin” (Reymond et al., 1996).

1.1.2 Molecular and functional characterization of remorin

Remorin has an intrinsically disordered N-terminal region and a conserved C-terminal domain (Fig. 1). Moreover, just like several other proteins, remorin also localizes to the PM in the cells of most plants (Watson et al., 2003; Nelson et al., 2006; Nohzadeh Malakshah et al., 2007). Several members of the remorin family across various plant species have been found in lipid rafts; lipid-enriched microdomains that are resistant to detergent action (Mongrand

et al., 2004; Laloï et al., 2007; Lefebvre et al., 2007).

The remorin gene is expressed in the embryonic, shoot apical, and vascular tissues of tomatoes (Bariola et al., 2004). In tobacco plants, the transcription of remorin increases with organ aging. The dehiscent tissues and other parts of tobacco leaves also express remorin (Raffaele et al., 2009a). The transcription and expression levels of some of the remorins are regulated by the abiotic stress-responses to adverse conditions such as cold weather, drought, and salt stress and by hormones including abscisic acid (ABA) and brassinolide (Nohzadeh Malakshah et al., 2007; Raffaele et al., 2007; Li et al., 2012a). Remorins are also associated with plant-microbe interactions, symbiosis, and pathogenesis (Fedorova et al., 2002; Wienkoop and Saalbach, 2003; Coaker et al., 2004; El Yahyaoui et al., 2004; Kistner et al., 2005; Widjaja et al., 2009). Additionally, the expression of remorin in *Arabidopsis* has been shown to be regulated by various biotic and abiotic stress-responses (Reymond et al., 2000; Raffaele et al., 2007). However, the remorin overexpressing cells and the remorin knockout cells do not show any noticeable phenotype (Reymond et al., 1996; Bariola et al., 2004).

Remorins are scaffold proteins that recruit various other signaling protein complexes to the lipid raft-enriched membrane regions, in order to

carry out the process of signal transduction (Jarsch and Ott, 2011). Moreover, AtREM1.3 shows a predominantly nuclear localization, when it is co-expressed with the IMPa proteins (Marin et al., 2012). Functionally, StREM1.3 was reported to interfere with the cell-to-cell movement of *Potato virus X* by directly binding to the TGBp1 virus movement protein (Raffaele et al., 2009b). MtREM2.2 was found to regulate the release of rhizobia into the host cytoplasm and interact with the symbiotic receptors, in order to control bacterial infection (Lefebvre et al., 2010). Recently, it was reported the *Arabidopsis* lines over-expressing *MiREM* showed an increased tolerance to osmotic stress (e.g., dehydration and salinity). As a response to this stress, the plants exhibited higher germination rates, increased seedling growth, and a higher activation of photosystem II (Checker and Khurana, 2013). Downregulation of PdREM increased the plant height, stem diameter, number of leaves, xylem size, and phloem zones, and also induced expression of cell wall biosynthesis- and microfibril angle (MFA)-related genes, whereas the overexpression of PdREM resulted into a diminished vegetative growth, in hybrid poplar lines. This indicates that *PdREM* might be contributing to the sheet strength and other properties of poplar wood (Li et al., 2013). The variable N-terminal region present in remorin, seems to confer functional

specificity to this protein (Raffaele et al., 2007).

1.1.3 Six groups of remorin family

Owing to significant differences, mainly in the N-terminal regions, the remorin family was subdivided into six separate groups. Group 1 comprises the canonical remorins with a Pro-rich N-terminal region. The group 1b proteins harbor the Remorin_N-terminal domains, and their N-terminal regions harbor twice as much as the Pro residues present in the group 1a remorins.

Group 2 remorins exist only in legumes and poplar trees. Interestingly, a group 2 remorin was identified during the transcriptome and proteome analysis of symbiotic interactions between legumes and rhizobial bacteria. The group 2 remorins MtSYMREM1 and LjSYMREM1, interact with the receptor-like protein kinases (RLKs) and localize to the infection threads within the nodular infection zone and the symbiosome membranes, respectively. Additionally, these proteins are required for bacterial infection (Lefebvre et al., 2010; Toth et al., 2012).

The group 3 remorins comprise short amino acid sequences and harbor a slightly more divergent C domain, in which a few conserved,

positively charged residues are replaced by aliphatic amino acids. The absence of an N-terminal domain implies that group 3 remorins can only perform the basic functions. Group 4 remorins harbor proline- and serine-rich N-terminal regions and the C-terminal domains of group 4 remorins are very similar to those of the group 1b remorins. The group 5 remorins harbor a relatively less proline-rich N-terminal region. They show a more divergent remorin_C-terminal domain as well as a highly variable N-terminal region. Owing to this reason, the functions of the group 5 remorins are difficult to predict. Group 6 remorins comprise relatively large proteins. The size of their N-terminal regions is variable, and these remorins could be further divided to several subgroups (Raffaele et al., 2007).

1.1.4 Intrinsically disordered N-terminal region

Remorin proteins are expected to harbor an intrinsically disordered N-terminal region. Generally, the intrinsically disordered proteins have an unstable folding structure under physiological conditions, so referred to naturally unfolded protein. The discovery of intrinsically disordered proteins led to a revision of the structure function paradigm, which states that a protein

can only fulfill its biological function by folding into a unique and structured state. Their importance is underlined by an exponential growth in the number of intrinsically disordered proteins described in literature in the last few decades (Sickmeier et al., 2007). The disordered proteins consist of amino acid sequences that are different from those of the ordered proteins. These proteins also differ in their flexibility, hydropathy, net charge, and several other factors and are significantly depleted in the bulky hydrophobic (isoleucine, leucine, and valine) and aromatic (tryptophan, tyrosine and phenylalanine) amino acid residues, which are highly represented in the hydrophobic core of globular proteins. The disordered proteins also possess fewer order promoting cysteine and asparagine residues and are substantially enriched in the polar amino acids (arginine, glutamine, serine, glutamate, and lysine, respectively), and in the structure-breaking glycine and proline residues. They also harbor a large number of alanine residues. All of the above-mentioned residues promote disorder in the protein structure (Cortese et al., 2008). The disordered proteins are often associated with the regulation of transcription, translation, cellular signal transduction, post-translational regulation, regulation of the self-assembly of large multi-protein complexes, and in the storage of small molecules (Dyson and Wright, 2005). Eighty-four

remorin proteins from six different groups possess an intrinsic disorder in their structure, with respect to their net charge and hydrophobicity. The N-terminal region of group 1b remorin proteins harbor disordered regions, as predicted by the PONDR VL-XT program (Marin and Ott, 2012). The N-terminal region of AtREM1.3 was described to be intrinsically disordered, and this region folded upon incubation with 2,2,2-trifluoroethanol, thereby suggesting that the disorder-to-order transition is induced by protein interaction (Marin et al., 2012). The analysis of the intrinsically disordered N-terminal regions of remorin may help us elucidate their roles in signal transduction.

1.1.5 The conserved C-terminal domain in remorin

All remorin proteins have highly conserved remorin C-terminal domains that include the coiled coil motifs necessary for homo-oligomerization and PM localization. A striking property of the Remorin_C-terminal domain is the high content of hydrophilic and charged residues. Some particularly conserved residues can be outlined as follows: Position 11 of Remorin_C is occupied by an aromatic residue (mainly tryptophan); positions 18, 22, and 25 by positively charged residues; and position 30 by an aliphatic residue for

all but one sequence. Position 33 harbors a tryptophan in all sequences, except in *Physcomitrella patens* and *Ceratopteris richardii*, and alanines are present in most remorin proteins at positions 75 and 80, respectively. Being highly conserved, these amino acids can be considered to be the identifying features of the remorin_C-terminal domain. In addition, a 23 amino acid-long sequence between the C-terminal residues 40 and 63 is predicted to show a coiled-coil structure, with a very high probability (Marcoils probability: 90 %). The prediction of the different positions in heptad repeats reveals the presence of aliphatic residues for sites a and d that form the core of the coiled-coil region. As compared to the coiled-coil domains of other proteins, these motifs in remorins consist of a higher number of charged residues (56 % for StREM1.3) in positions b, c, d, and e, respectively. This characteristic could be responsible for the highly stable protein interactions mediated by this domain (Raffaele et al., 2007). Recently, it was reported that a domain of 28 residues at the C-terminus of the potato StREM1.3 is required for the PM recruitment, and was named as the Remorin_C-terminal anchor (RemCA) domain (Perraki et al., 2012). This domain adopts an alpha-helical conformation in polar environments. It directly binds to lipids and biological membranes, with higher affinity for the negatively charged lipids abundant in

detergent insoluble membranes. Mutations in the RemCA domain abolish StREM1.3 PM binding as well as the function of StREM1.3 in the suppression of potato virus X propagation. No plant proteins outside of the remorin family harbor RemCA-homologous domains. However, the RemCA domain shares bias in its amino acid composition and predicted structural fold with the membrane binding domains of bacterial, viral, and animal proteins. These previously reported results suggest that the RemCA domain does not originate from an ancestral membrane-binding domain shared with lineages beyond the plant kingdom. The emergence of the RemCA domain by convergent evolution among unrelated membrane binding domains seems likely (Perraki et al., 2012).

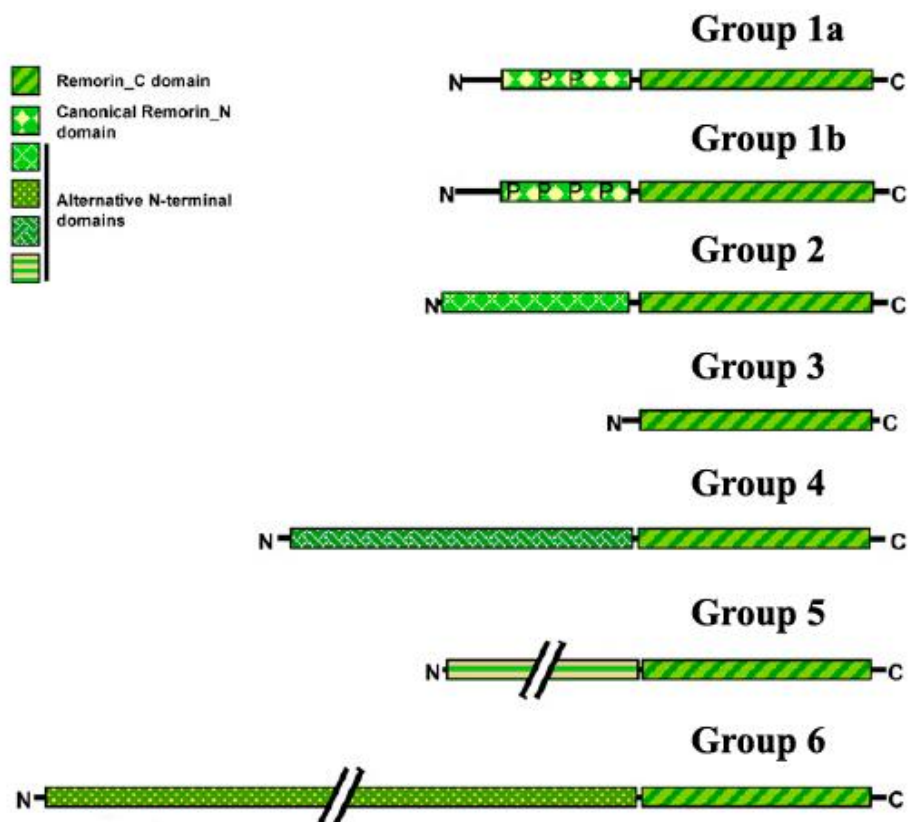


Figure 1. Six groups and protein domains of the remorin family. The diagrams are based on a previous report (Raffaele et al., 2007). In the diagrams, domain lengths are proportional to the average protein sequence length (except for groups 5 and 6, for which the representation of the N-terminal region is intercepted by “//” indicating a variable length of this module within these 2 groups).

1.2 Plasma membrane partitioning

1.2.1 Plasma membrane

The plasma membrane (PM) comprising the phospholipid bilayer and anchored proteins is a biological membrane that separates the interior of all cells from the outside environment. The PM is a fluid and selectively permeable membrane that allows the selective passage of certain substances, while blocking other unwanted substances. Its basic function is to protect the cell from its surroundings. Moreover, the PM is involved in cell adhesion, ion conductivity, and cell signaling, and it serves as an attachment surface for various different extracellular structures, including the cell wall and the cytoskeleton. The lateral compartmentalization of the PM helps organize the diverse organelles inside the cell, by spatially restricting the interactions between specific sets of proteins, as well as between proteins and specific membrane lipids (Boutte and Moreau, 2014).

1.2.2 Microdomain of plasma membrane

Plasma membranes are highly organized structures that are partitioned into areas of distinct composition, structure, and function, known as

microdomains (Malinsky et al., 2013). For example, according to some reports, the basolateral membrane of root epidermal cells is targeted by the polarly localized PIN-FORMED auxin efflux carrier PIN2 (Muller et al., 1998), by the focal accumulation of the MILDEW RESISTANCE LOCUS O protein at perihaustral membranes during plant-microbe interactions (Bhat et al., 2005), and by the casparyan strip that are marked with CASP proteins (Roppolo et al., 2011). However, most of these are further subdivided. Increasing evidence suggests that the large unit that is between 40 and 300 nm in diameter and enriched in membrane proteins, does not freely diffuse inside the PM bilayer. This region is preassembled into distinct subdomains (Kusumi et al., 2012). Lipid rafts that are characteristically enriched in sterols and sphingolipids, can be found within these compartments. The interaction of raft-localized proteins and scaffolds can lead to the clustering of nanoscale domains into larger units, defined as raft platforms or membrane microdomains (Lingwood and Simons, 2010). These domains are usually a few microns in size and are believed to harbor defined sets of preassembled signaling protein complexes, including components of the innate immune system (Jarsch et al., 2014). Microdomains have been implicated in regulating a wide variety of cellular processes. However, their exact role in

the process of signal transduction remains elusive.

1.2.3 Microdomain-associated proteins

A number of cell studies have revealed the presence of membrane-associated proteins such as remorins (Konrad et al., 2014), flotillins (Haney and Long, 2010; Li et al., 2012b), the potassium channel KAT1 (Reuff et al., 2010), the anion channel SLAH3 (Demir et al., 2013), the LysM receptor LYK3 (Haney et al., 2011), the NADPH oxidase RBOHD (Lherminier et al., 2009), and the exocyst protein SECA3 (Zhang et al., 2013). Remorins were suggested to play a role as molecular scaffold proteins that mediate the assembly and localization of subcellular protein complexes. The localization of single remorins to membrane domains has been shown in the case of the ectopically expressed REM1.3 from potato (*Solanum tuberosum*), for an endogenous Remorin from tomato (*Solanum lycopersicum*), as well for the closely related protein from the Arabidopsis genus (REM1.3/At2g45820) (Jarsch et al., 2014). Moreover, Arabidopsis remorins such as AtREM1.2/1.3 have been used as membrane domain markers (Demir et al., 2013)

1.3 Scaffold protein

1.3.1 Definition of scaffold

The location of the proteins inside the cell and the kinetics of their activation are important in signaling transduction pathways. Scaffold proteins are crucial regulators in many important signaling pathways. However, scaffolds are not strictly defined in function. Recently, an attempt was made to define scaffolds as molecules that bind to at least two other signaling proteins to regulate their action (Shaw and Filbert, 2009; Buday and Tompa, 2010).

Scaffold proteins bind to various other proteins. However, they display no enzymatic activity, as their primary function is to mediate the interactions between other proteins. Central to this definition is the ability of scaffold proteins to regulate signal transduction and, in most cases, to localize signaling molecules at specific areas of the cell, such as the plasma membrane, the cytoplasm, the nucleus, the Golgi, the endosomes, and the mitochondria.

1.3.2 Function of scaffold protein

Scaffold proteins assemble the signaling components, localize the signaling

molecules to subcellular compartments, coordinate the positive and negative feedback signals, and protect the activated signaling molecules from competing proteins (Shaw and Filbert, 2009). The most basic function of scaffold proteins is to tether the signaling components into complexes. This assembly could improve the efficiency by concentrating the signaling components in a small volume, thereby increasing the specificity by preventing unnecessary interactions between signaling proteins. For example, some scaffolds mediate specific kinase-substrate phosphorylation. Moreover, some signaling proteins need multiple interactions for activation. Scaffold proteins may be able to mediate signaling complexes, and this results into multiple modifications (Levchenko et al., 2000). Scaffolds could also cause allosteric changes in the signaling protein that either enhance or inhibit the cascade (Burack and Shaw, 2000). They are able to localize the signaling reaction to a specific area in the cell. This is important for the local production of signaling intermediates. For example, A-kinase anchor proteins (AKAPs) cause the local phosphorylation of cyclic AMP-dependent protein kinase (PKA) at various sites (Wong and Scott, 2004). Scaffold proteins can potentially display other functions that coordinate the positive and negative feedback. Scaffolds bind all three kinases (MAPKKK, MAPKK and MAPK)

involved in signaling cascades, and this significantly enhances the kinase specificity by restricting signal amplification and by limiting kinase phosphorylation to only one downstream target (Levchenko et al., 2000; Locasale et al., 2007). Protecting the activated signaling molecules from inactivation is an important task. Scaffolds have been proposed to protect activated signaling molecules from inactivation and/or degradation. Mathematical modeling has shown that kinases in a cascade devoid of scaffolds have a higher probability of being dephosphorylated by phosphatases even before they phosphorylate their corresponding downstream targets (Locasale et al., 2007).

1.3.3 Homer scaffold protein

It was assumed that remorins would behave like the homer scaffold proteins (Jarsch and Ott, 2011). The Homer family of adaptor proteins in mammals consists of three members, viz. Homer1, Homer2, and Homer3, all of which have several isoforms as a result of alternative splicing (Shiraishi-Yamaguchi and Furuichi, 2007). The homer proteins harbor an N-terminal target-binding region that includes the EVH1 domain (which binds to the proline-rich regions in the interacting proteins), and a C-terminal self-assembly region

that includes a coiled-coil domain and a leucine zipper motif (Shiraishi et al., 2004). Homers function to aggregate receptors (such as the metabotropic glutamate receptors), and signaling proteins at the neurological synapse (Thomas, 2002). In addition, they can also modulate calcium signaling downstream of the glutamate receptor in neuronal cells by linking it with the inositol-1,4,5-trisphosphate receptors in the endoplasmic reticulum (Xiao et al., 2000). Homer interacts with various partner proteins (e.g., the glutamate, NMDA, and α -amino-3- hydroxyl-5-methylisoxazole-4-propionate receptors, respectively) and is therefore expected to exhibit functional diversity. Whereas the Homer 1b/c proteins physically interact only with the glutamate receptor, they interconnect and recruit these proteins into close proximity with each other by interacting with some of their downstream targets (e.g., dynamin3, PSD95, and SHANK), thereby leading to the assembly of a functional signaling complex (Lu et al., 2007).

1.4 Purpose of the study

Remorin, a plant-specific protein comprising an intrinsically disordered N-terminal region and a conserved C-terminal domain, is known to play a role in various biotic and abiotic stress-responses elicited by external stimuli such as host-microbe interactions. However, its function is not well understood. Therefore, the main purpose of this study is to elucidate the role of remorin in soybean and *Arabidopsis*. I have adopted both genetic as well as biochemical approaches in order to elucidate its function, and to highlight the signaling pathways involved. In chapter I, I have examined the biologically distinct roles of GmREM1.1 and GmREM2.1 during the root nodule development of soybean. In the chapter II, I have attempted to elucidate the biological function and signaling pathways of AtREM4s during the geminivirus infections in *Arabidopsis*.

CHAPTER I.

**GmREM1.1 and GmREM2.1, which
encode the remorin proteins in soybean,
have distinct roles during root nodule
development**

2.1 Abstract

Remorin is involved in various biotic and abiotic stresses, including host-microbe interactions. To elucidate its roles during root nodule development, I characterized remorin genes in soybean. The genes belonging to groups 1 and 2 were both expressed during root nodule development but with somewhat different temporal patterns. Using a biochemical assay, I showed that the homo-oligomerization of GmREM1.1 was mediated by the coiled-coil region in the C-terminal domain in combination with either the N-terminal or C-terminal anchor peptides (RemCA). Plasma membrane targeting was also sufficiently mediated by RemCA from GmREM1s but not from GmREM2.1. In addition, *GmREM1.1* was highly expressed in the nodule primordia and inner cortex region of root nodules, whereas *GmREM2.1* transcription was mainly detected in the infected cells during nodule development. Moreover, *RNAi-GmREM2.1* hairy roots showed significantly reduced nodule formation, but *RNAi-GmREM1.1* had little effect on nodule formation. Taken together, these results suggest that GmREM1.1 and GmREM2.1, with different molecular features, function distinctively during root nodule development.

2.2 Introduction

Globally, soybean (*Glycine max*) is an important crop for food and as a biofuel source. Due to the capacity to interact with nitrogen-fixing soil bacteria called rhizobia, soybean can form new root structures named nodules. Legume roots secrete flavonoid compounds to induce the transcription of bacterial nodulation genes involved in the synthesis and secretion of Nod factors (Zuanazzi et al. 1998). During symbiosis, the host plant gains access to fixed nitrogen from the bacteria in exchange for carbon sources (Desbrosses and Stougaard 2011). Soybean develops spherical, determinate root nodules with a central infection zone composed of infected cells that are responsible for N₂ fixation and N₂ assimilation and uninfected cells where ureide synthesis occurs (Collier and Tegeder, 2012).

Multiple remorin genes are present in all land plants and are involved in various biotic and abiotic stress responses (Jarsch and Ott, 2011). The remorin proteins consist of a variable N-terminal region that is responsible for functional divergence and a conserved C-terminal region that is associated with oligomerization and localization to the plasma membrane (PM) (Raffaele et al., 2007; Marin and Ott, 2012). A recent report showed that the short C-terminal

anchor region (RemCA) is essential for PM targeting (Perraki et al., 2012), and S-acylation of cysteine residues in the C-terminal hydrophobic core contributes to the membrane association of remorin proteins (Konrad et al., 2014). The remorin family is divided into six groups according to the variable N-terminal structures (Raffaele et al., 2007). Remorins are expressed in diverse tissues (Bariola et al., 2004) and are regulated by various biotic and abiotic stresses (Nohzadeh Malakshah et al., 2007; Raffaele et al., 2007; Li et al., 2012a). Previous research has revealed that remorin is largely involved in plant-microbe interactions. For example, potato StREM1.3 interacted with the viral protein TGBp1 from potato virus X (Raffaele et al., 2009b) and inhibited TGBp1's ability to increase plasmodesmata permeability (Perraki et al., 2014). *Arabidopsis* AtREM1.3 was differentially phosphorylated after bacterial elicitor treatments (Benschop et al., 2007), and AtREM1.2 was identified as a component of the RIN4 protein complex that regulates the stomatal aperture against pathogen attack (Liu et al., 2009). In addition, REM1.3 was revealed to enhance susceptibility to *Phytophthora infestans* (Bozkurt et al., 2014). Moreover, group 2 remorins are strongly induced during symbiotic interactions between legumes and rhizobia. As group 2 remorins, MtSYREM1 from *Medicago truncatula* and LjSYREM1 from *Lotus japonicus* interacted with

symbiosis-related receptor-like kinases (RLKs) and regulated nodule development (Lefebvre et al., 2010; Toth et al., 2012). However, their exact biological function during the plant-microbe interaction remains elusive.

To date, most remorin studies have focused on only a few plant species, including tomato, potato, and *Arabidopsis*. Soybean remorin was first reported in the 1990s (Reymond et al., 1995). However, subsequent reports on soybean remorin are scarce. Thus, in this study, as a first step in elucidating the role of remorin in soybean, I showed that *GmREM1.1* and *GmREM2.1* have different protein structures for localization and oligomerization and function distinctively during nodule development.

2.3 Materials and methods

2.3.1 Plant materials and bacterial strains

Soybean (*Glycine max*) seeds were surface-sterilized with a hydrogen peroxide/ethanol solution [3% (w/w) hydrogen peroxide, 70% (v/v) ethanol] for 3 min and rinsed at least five times with an excess amount of distilled water. Seeds were placed into wet vermiculite at a depth of 1-2 cm and grown in a growth room (16 h/8 h light/dark cycle, 27°C). The *Bradyrhizobium japonicum* USDA110 strain was used to nodulate soybean seedlings or transgenic hairy roots of composite plants, and the inoculation process was performed as previously described (Lee et al., 2004).

2.3.2 Plasmid construction

Truncated *GmREM1.1* fragments for the yeast two-hybrid assay were amplified from a full-length *GmREM1.1* cDNA clone as a template using the primer pairs listed in supplementary Table 2. Amplified fragments were ligated in frame into the pGAD GH and pGBT9 BS vectors between the *SpeI* and *SalI* sites. For the bimolecular fluorescence complementation (BiFC) assay, full-length or truncated *GmREM* PCR products were subcloned into the pSPYNE173 and

pSPYCE(MR) vectors (Waadt et al., 2008). To analyze subcellular localization in tobacco epidermal cells, all tested fragments were C-terminally fused with green fluorescent protein (GFP) in the pCAMBIA 1303 vector (CAMBIA, Australia). For promoter-GUS constructs, 1,615-bp (*GmREM1.1*) or 1,500-bp (*GmREM2.1*) upstream regions were amplified from soybean genomic DNA and finally cloned into the gateway pBGWFS7 (for *GmREM1.1*; Karimi et al. 2002) or pCAMBIA1303 (for *GmREM2.1*) vectors, resulting in transcriptional fusion with the GUS reporter. To silence *GmREM2.1*, a 178-bp fragment of the *GmREM2.1* coding region was amplified and subcloned into the pENTR-D/TOPO vector (Invitrogen, USA). By gateway LR recombination, the fragment was finally introduced into the pK7GWIWG2D(II) vector (Karimi et al., 2002).

2.3.3 Yeast two-hybrid assay

The yeast strain pJ69-4A was simultaneously transformed with the pair of bait and prey recombinant plasmids by the PEG/LiAc method as described previously (Gietz et al., 1992). Transformants were plated on minimal SD medium containing dropout supplements without leucine or tryptophan. The selected double transformants were transferred and grown in the absence of

adenine, histidine, leucine, and tryptophan to select interactors. For the serial dilution assay, yeast cells were harvested and adjusted to an $OD_{600}=0.5$ with sterilized double-distilled water and diluted to 1/10, 1/100, and 1/1,000. A total of 2 μ L of diluted yeast cells was spotted onto selection medium as previously described (Lee et al., 2009).

2.3.4 Bimolecular fluorescence complementation (BiFC) and localization of GFP-conjugated proteins

The constructs were transformed to *Agrobacterium tumefaciens* strain GV3101 and infiltrated into leaf epidermal cells of 5-week-old tobacco plants (*Nicotiana benthamiana*). The BiFC assay was performed as previously described (Voinnet et al., 2003). For the localization of GFP-conjugated proteins, the GV3101 strains contained each construct at an $OD_{600}=0.5$, and another GV3101 strain containing a virus-encoded suppressor, p19 protein, was co-infiltrated to prevent the onset of post-transcriptional gene silencing. Fluorescence detection was performed at 3 days after infiltration using the LSM700 confocal laser scanning microscope (Carl Zeiss, Germany).

2.3.5 Generation of transgenic hairy roots and nodules

Recombinant plasmids were introduced into *A. rhizogenes* K599 using the freeze-thaw method (Hofgen and Willmitzer, 1988). Composite plants with transgenic hairy roots were generated as previously described (Collier et al., 2005) with minor modifications. Briefly, 2-week-old soybean shoots were cut between the trifoliate and true leaves and placed into 8-cm³ rockwool blocks that were saturated with 4-5 mL of *A. rhizogenes* cells, which were resuspended in 1/4x MS medium (pH 5.8) to an OD₆₀₀=0.3. Covered with clear plastic domes, the shoot segments were incubated in a growth room (16 h/8 h light/dark cycle, 25°C) until the plants were fully wilted. The blocks were periodically saturated with B&D solution (Kereszt et al., 2007) for approximately 3 weeks until hairy roots emerged outward from the blocks. Then, the rockwools were removed using forceps, and GFP-expressing transgenic hairy roots were analyzed using a Lumar V12 stereomicroscope equipped with epifluorescence GFP excitation and emission filters (Carl Zeiss,

Germany).

2.3.6 Histochemical GUS analysis

The GUS histochemical assay was performed according to the method of Stomp (1992). Transgenic hairy roots were submerged in GUS staining solution (0.1 M sodium phosphate buffer pH 7.0, 0.1% Triton X-100, 10 mM EDTA, 0.5 mM K₃Fe(CN)₆, 0.5 mM K₄Fe(CN)₆, 250 µM X-Gluc) and incubated at 37°C overnight. After incubation, the samples were cleared with 100% ethanol and stored in 70% ethanol after the imaging process. For thin sections, GUS-stained root and nodule samples were embedded in Technovit 7100 (Kulzer GmbH, Germany), and 5-µm-thick sections were obtained using a rotary microtome (American Optical, USA). The sections were then placed on the slides and observed using a bright field microscope (Carl Zeiss, DE/Axio Imager A1, Germany).

Table 2. Primers used for constructs.

Gene	Purpose	Primers (5' → 3')	
GmREM1.1	Localization	F	CCATGGCAGAGCTCCAAA
		R	ACTAGTAAAGCATCCAAAGGCCTTC
GmREM1.1N	Localization	F	CCATGGCAGAGCTCCAAA
		R	ACTAGTCTCTTCTCTATTCTGCAAGAG
GmREM1.1C	Localization	F	CCATGGTAAAACGATTGTCTAATGTGA
		R	ACTAGTAAAGCATCCAAAGGCCTTC
GmREM1.1Δ	Localization	F	CCATGGTAAAACGATTGTCTAATGTGA
		R	ACTAGTACGCTTGGCTTCAACCATT
GmREM1.1CA	Localization	F	CCATGGGTGAAGAAATTCTCAAG
		R	ACTAGTAAAGCATCCAAAGGCCTTC
GmREM1.3CA	Localization	F	CCATGGGGAAAGATCTTCTTAAG
		R	ACTAGTGAACAAACCAAGGAGTTCTT
GmREM2.1	Localization	F	CCATGGGAGTATCGGGGAACC
		R	ACTAGT ACTGCTGCCGAAGCATG
GmREM2.1CA	Localization	F	CCATGGGAGAAGAATTCTTAGAAA
		R	ACTAGT ACTGCTGCCGAAGCATG
GmREM1.1	Y2H	F	ACTAGTGTGGCAGAGCTCCAAAC
		R	GTCGACTTAAAGCATCCAAAGG
GmREM1.1N	Y2H	F	ACTAGTGTGGCAGAGCTCCAAAC
		R	GTCGACTTACTCTTCTATTCTGCA
GmREM1.1C	Y2H	F	ACTAGTGAACGATTGTCTAATGTGAAG
		R	GTCGACTTAAAGCATCCAAAGG
GmREM1.1Δ	Y2H	F	ACTAGTGTGGCAGAGCTCCAAAC
		R	GTCGACTTAACGCTTGGCTTCAACCATT
GmREM1.1CA	Y2H	F	ACTAGTGAACGATTGTCTAATGTGAAG
		R	GTCGACTTAACGCTTGGCTTCAACCATT
GmREM1.1CA	Y2H	F	ACTAGTGGGTGAAGAAATTCTCAAGG
		R	GTCGACTTAAAGCATCCAAAGG
GmREM1.3	Y2H	F	ACTAGTGTGACAGAAGAACCAAACCAA
		R	GTCGACTTAGAAACAACCAAGGAGTTT

GmREM2.1	Y2H	F	ACTAGTGATGGAGTATCGGGGAAC
		R	GTCGACTTAACTGCTGCCGAAGCAT
GmREM1.1	BiFC	F	ACTAGTGATGGCAGAGCTCCAAAC
		R	GTCGACAAAGCATCCAAAGG
GmREM1.1N	BiFC	F	ACTAGTGATGGCAGAGCTCCAAAC
		R	GTCGACCTCTTCTCTATTCTGCA
GmREM1.1C	BiFC	F	ACTAGTATGAAACGATTGTCTAATGTGA
		R	GTCGACAAAGCATCCAAAGG
GmREM1.3	BiFC	F	ACTAGTATGACAGAAGAACAAACCAA
		R	GTCGACGAAACAACCAAGGAGTTTC
GmREM2.1	BiFC	F	ACTAGTATGGAGTATCGGGGAAC
		R	GTCGACACTGCTGCCGAAGCAT
GmREM1.1 P	Promoter	F	CACCGGCTGTAAATCGTCATCAAT
		R	AGCTTCGGAGTTGGITCGG
GmREM2.1 P	Promoter	F	GGATCCTAAAAAGCAAAAAAGCTAG
		R	ACTAGTCCCATAACGTATAACACACTT

2.4 Results

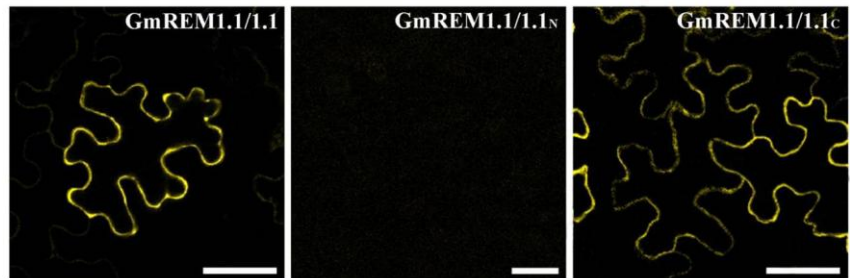
2.4.1 Intra- and intergenic protein-protein interactions of GmREMs

GmREM1.1 was originally isolated as an upregulated cDNA clone in the root nodules of soybean (Lee et al. 2004), and a specifically expressed clone in root nodules was also isolated and named *GmREM2.1* (An, unpublished) due to its close relationships with *MtSYREMI* and *LjSYREMI* (Lefebvre et al. 2010; Toth et al. 2012). *GmREM1.1* showed a high degree of similarity to other plant remorins belonging to group 1 and possessed two conserved domains in their proline-rich N-terminal (Remorin_N; PF03766) and coiled-coil motif-containing C-terminal regions (Remorin_C; PF03763). However, *GmREM2.1* harbored only a conserved Remorin_C domain, and its N-terminal region contained few proline residues and showed no significant homology to those of group 1 remorins; these traits are typical for members of the group 2 remorin family (An, unpublished).

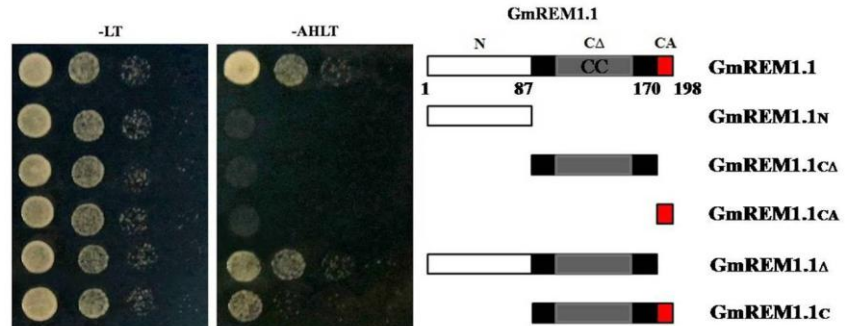
Cross-linked GmREM1.1-1.4 existed in various oligomeric forms (Son et al. 2010). To confirm this data *in planta*, I performed a BiFC assay using transiently expressed GmREM1.1 in *N. benthamiana* leaves. Strong YFP

signals were detected in the plasma membrane (PM) of epidermal cells when GmREM1.1 was co-expressed with the full-length or C-terminal domains of GmREM1.1, but no signal was detected with the N-terminal domain (Fig. 2-1A). Thus, I examined which regions mediated this homo-oligomerization by a yeast two-hybrid assay using the full-length and truncated versions of GmREM1.1. Full-length GmREM1.1 protein bound to GmREM1.1 Δ (amino acids 1–170) and GmREM1c (amino acids 88–198) fragments, but did not interact with GmREM1.1N (amino acids 1–87), GmREM1.1c Δ (amino acids 88–170), or GmREM1.1c Δ (amino acids 171–198) in yeast (Fig. 2-1B). Furthermore, because the C-terminal regions of GmREMs were highly conserved regardless of group, we tested whether oligomeric structures could form between different GmREMs *in planta*. As shown in Figure 2-1C, whereas hetero-oligomers between GmREM1.1 and GmREM1.3 formed, GmREM2.1 could not exist as an oligomer with GmREM1.1 and GmREM1.3, except as a homo-oligomeric structure.

A



B



C

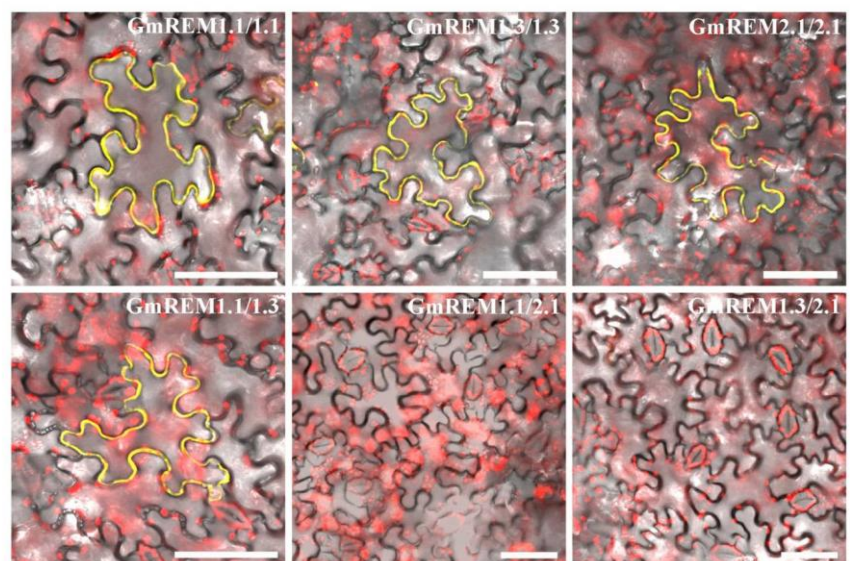


Figure 2-1. Determination of essential domains for GmREM1.1

dimerization and physical interactions between GmREM1.1/1.3/2.1. (A)

The dimerization of GmREM1.1 with its the N- or C-terminal fragment was analyzed by a BiFC assay in *N. benthamiana*, as described in the Materials and Methods section. (B) Individual truncated GmREM1.1 (GmREM1.1, GmREM1.1_N, GmREM1.1_{CΔ}, GmREM1.1_{CA}, GmREM1.1_Δ, and GmREM1.1_C) was cotransformed with full-length GmREM1.1 into yeast cells, and a serial dilution assay was performed. Numbers indicate amino acid positions. CC, predicted coiled-coil region (amino acids 110–151). (C) Physical interactions for the indicated GmREMs were assessed using split YFP assays. Scale bar = 50 μm.

2.4.2 A short C-terminal anchor targets GmREM1.1 and GmREM1.3 to the PM

Recently, the RemCA region of StREM1.3 was identified as a necessary and sufficient region for localizing StREM1.3 to the PM (Perraki et al., 2012), and several remorin proteins from other species are targeted to the PM by this short peptide (Konrad et al., 2014). As shown in previous results, RemCA sequences were also found in GmREMs, and dimeric forms of GmREMs were clearly localized in the PM. Thus, I examined the involvement of RemCA in GmREM localization using transiently expressed GFP-conjugated GmREMs. While full-length GmREM1.1 and GmREM1.1C were targeted to the PM, GmREM1.1N and GmREM1.1C Δ without RemCA were largely detected in the cytosol (Fig. 2-2A). Moreover, when only the RemCA regions of GmREM1.1 and GmREM1.3 were expressed, strong signals were detected in the PM (Fig. 2-2A). In contrast, RemCA from GmREM2.1 was not significantly targeted to the PM, although its full-length protein clearly localized to the PM (Fig. 2-2B).

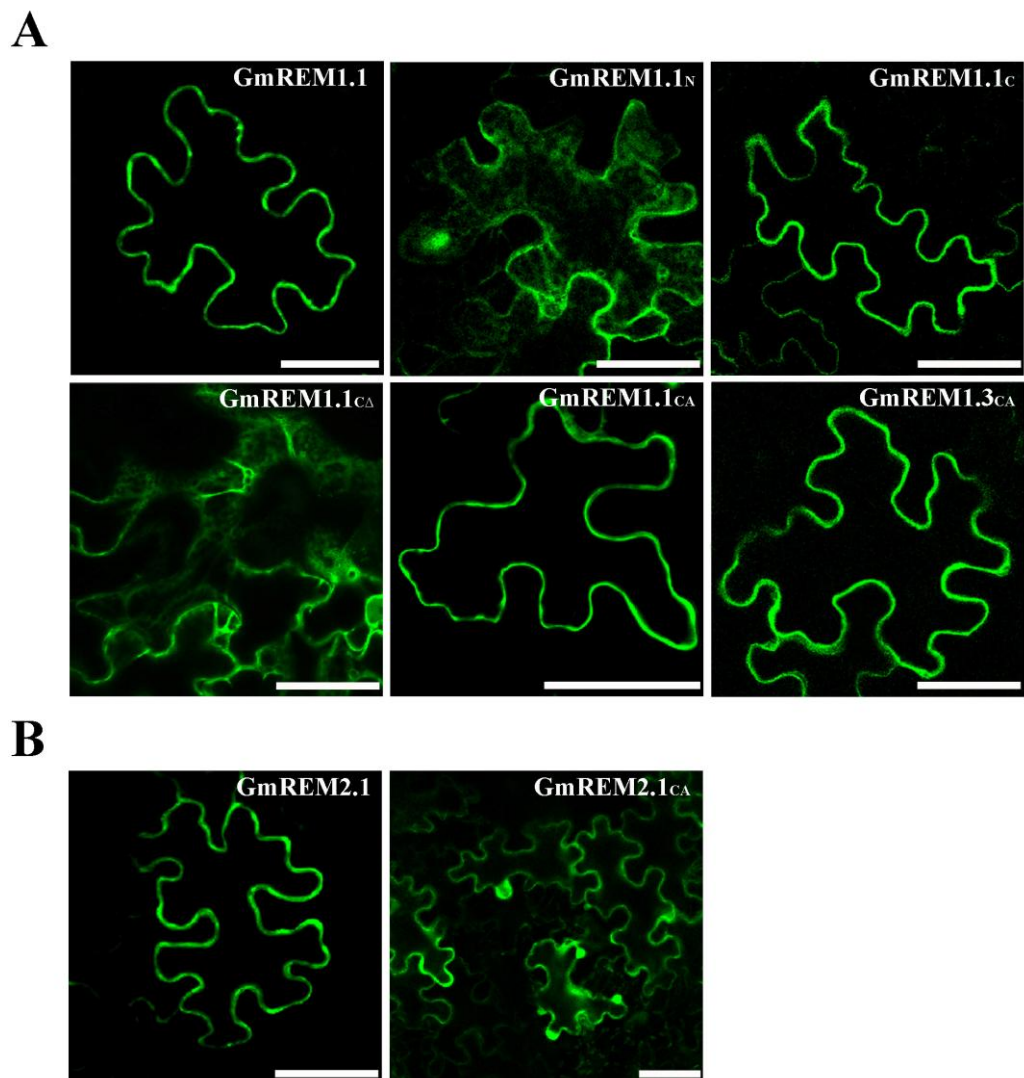


Figure 2-2. The plasma membrane targeting of GmREM1.1/1.3/2.1.

Tobacco epidermal cells transiently expressing GmREM1.1, GmREM1.1_N, GmREM1.1c, GmREM1.1_Δ, GmREM1.1CA, GmREM1.3CA (A), GmREM2.1,

and GmREM2.1CA (B) were observed by confocal laser scanning microscopy.

GmREM1.1 constructs are shown in Figure 2-1. Scale bar = 50 μ m.

2.4.3 *GmREM1.1* and *GmREM2.1* have distinct spatial expression patterns in root nodules

To investigate the detailed expression patterns of the *GmREMs* during nodule development, we performed a promoter analysis using root nodules on transgenic hairy roots containing *GmREM1.1::GUS* or *GmREM2.1::GUS* constructs. *GmREM1.1* was highly expressed at the cortex region in uninoculated roots (Fig. 2-3A and D). At 10 day after inoculation (DAI) with *B. japonicum*, strong GUS signals were detected at the emerging nodule primordia (Fig. 2-3B). However, the GUS signal significantly disappeared in 4 WAI nodules (Fig. 2-3C). Unlike *GmREM1.1*, the *GmREM2.1* promoter activity was extremely nodule-specific during nodule development (Fig. 2-3E and G). For close observation, GUS-stained nodule samples were thin-sectioned, and images were obtained using microscopy. The GUS signal of *GmREM1.1* was highly detected in the inner cortex region similar to that in the root (Fig. 2-3G and E), whereas *GmREM2.1* was mainly expressed in the infected cells with lower levels in the cortex (Fig. 2-3I and J). These spatiotemporally separated expression patterns between *GmREM1.1* and *GmREM2.1* also suggest their distinct roles in nodule development.

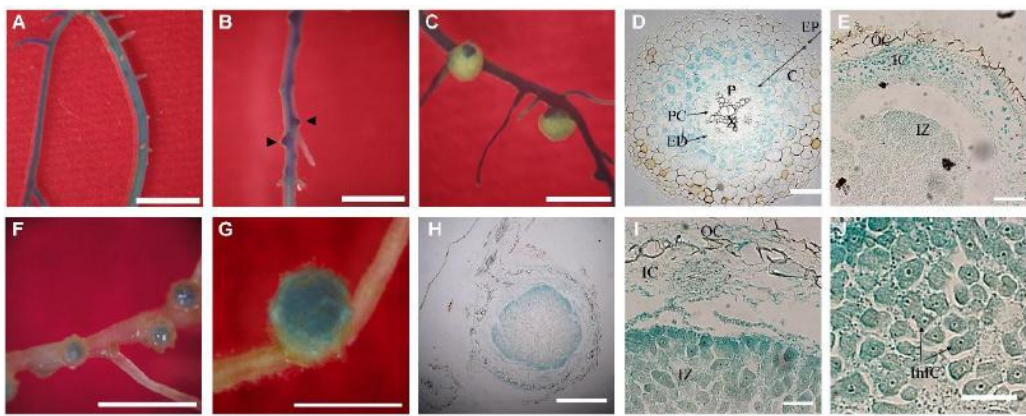
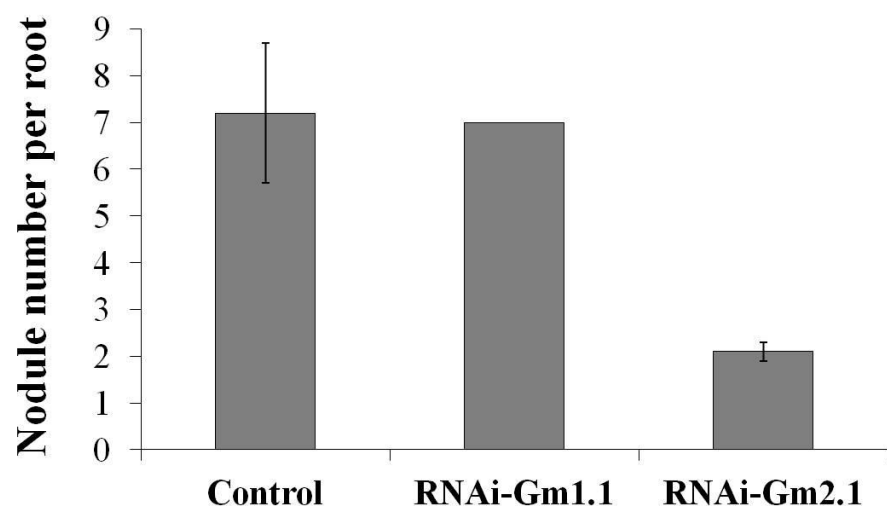


Figure 2-3. Promoter analysis of *GmREM1.1/2.1*. Histochemical GUS analysis of transgenic hairy roots and nodules expressing *GmREM1.1::GUS* (A-E) and *GmREM2.1::GUS* (F-J). (A) 2 days after YEM medium treatment, (B) 10 DAI, and (C) 4 WAI. (D-E) Transverse sections of transgenic hairy root (D) and root nodules (E) harboring *GmREM1.1::GUS*. (F) 2 WAI and (G) 3 WAI. (H-J) Transverse sections of 3 WAI (H) and 5 WAI root nodules (I-J) harboring *GmREM1.1::GUS*. Arrowheads indicate the developing nodule primordium. EP, epidermis; C, cortex; ED, endodermis; PC, pericycle; P, phloem; X, xylem; OC, outer cortex; IC, inner cortex; IZ, infected zone; InfC, infected cells. Bars = 5 mm (A, B, C, F, G), 1 mm (H), and 100 μ m (D, E, I, J).

2.4.4 Silencing of *GmREM2.1* leads to decreased nodule formation

To functionally test the roles of *GmREM1.1* and *GmREM2.1* during nodule development, transgenic hairy roots harboring RNAi-mediated silencing constructs were generated and subjected to the nodulation assay. At 3 weeks post-inoculation with *B. japonicum*, GFP-expressing mature nodules on transgenic hairy roots were screened under a fluorescence microscope and subjected to statistical analyses. The total nodule number was much lower in the *GmREM2.1*-silenced transgenic roots compared to the empty vector control, whereas little effect on nodulation was observed in *GmREM1.1*-silenced composite plants (Fig. 2-4A). In addition, approximately 30% of the transgenic roots of *RNAi-GmREM2.1* had impaired nodulation in contrast to the 5% of transgenic roots in the vector control line (Fig. 2-4B), indicating that *GmREM2.1* must participate in nodule formation.

A



B

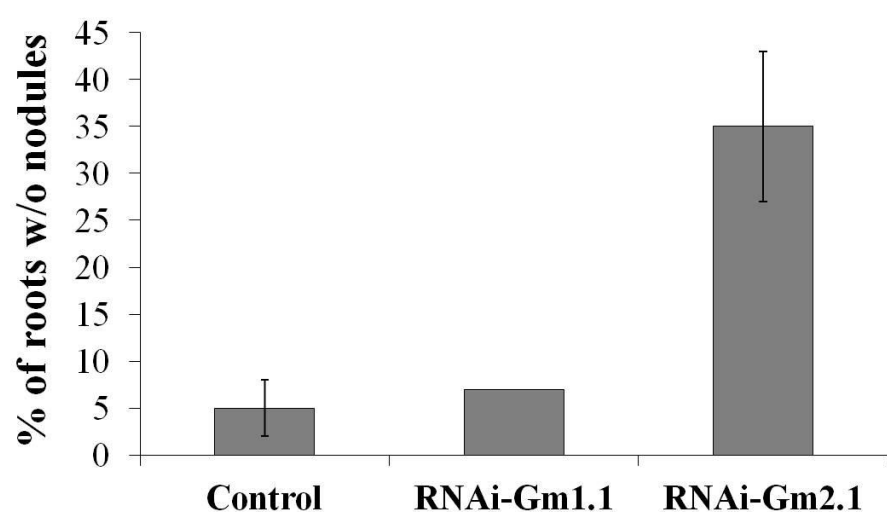


Figure 2-4. The total nodule numbers of *GmREM*-silenced transgenic roots.

(A) Mature nodules were counted at 3 weeks after *B. japonicum* inoculation.

(B) The ratio of transgenic hairy roots without nodules was calculated at 3 weeks after *B. japonicum* inoculation. For experimental reliability, short transgenic roots (< 5 cm) were excluded from statistics for the possibility of delayed emergence and rhizobium infection. In each experiment, 18 to 25 transgenic roots from at least 5 plants were analyzed. Transgenic hairy roots harboring empty vector were used for the control, and error bars represent the standard error of the mean values from three independent biological replicates.

2.5 Discussion

Most lines of evidence regarding the putative roles for group 1 remorins implicate remorins as a modulator that regulates cell surface signaling and microbe residence during plant-pathogenic microbe interactions (Raffaele et al., 2007; Jarsch and Ott, 2011; Bozkurt et al., 2014). For group 2 remorins, MtSYREM1 and LjSYREM1 are present on the infection thread in the nodule infection zone, and both proteins have abilities to bind with several RLKs involved in the early nodulation process, such as LYK3, DMI2, and NFR1 (Lefebvre et al., 2010; Toth et al., 2012). However, no integrated study has used multiple genes or different group members for a defined plant response. Moreover, despite its importance as an economically valuable crop species, no previous study on remorin genes in soybean has been reported. In this study, I demonstrated molecular characteristics and putative roles of remorin genes expressed in soybean root nodules during nodule development.

GmREM1.1 and GmREM2.1 have different characteristics of oligomerization and PM targeting

GmREM1.1 and *GmREM2.1*, classified into two different evolutionary groups,

have typical remorin N- (only for GmREM1s) and C-terminal domains with a coiled-coil motif and RemCA peptides. In agreement with previous reports (Kohn et al., 1997; Bariola et al., 2004; Perraki et al., 2012), GmREM1.1 can exist in oligomeric forms via an intact C-terminal region *in planta* (Fig. 2-1A). However, the yeast binding assay revealed that the coiled-coil region (between amino acids 110–151 in GmREM1.1) was necessary but not sufficient for oligomerization (Fig. 2-1B). In fact, either the N-terminal or RemCA region was indispensable for stable interaction (Fig. 2-1B), in agreement with the reports that the AtREM1.3 N-terminal region facilitates stable homo-oligomerization (Martin et al. 2012). Like AtREM1.3, incidental structural regions of GmREM1.1 that cooperate with the core coiled-coil region might contribute to the proper conformational change for protein-protein interactions.

Next, based on the sequence similarities and overlapping expression patterns, I hypothesized that different GmREMs could form hetero-oligomers as well as homo-oligomers and tested this possibility *in planta* using the BiFC assay. Interestingly, whereas apparent physical interactions occurred between intragroup members, no significant signals could be detected between the intergroup members (Fig 2-1C). This result might be because GmREM2.1 did not contain the well-defined remorin N-terminal domain and the relatively low

sequence identity with GmREM1 in its RemCA motif. To support this assumption, additional approaches, such as domain swapping or a binding assay with mutated version of the proteins, are needed.

A short C-terminal anchor region known as RemCA is indispensable and sufficient for targeting remorins to the PM (Perraki et al., 2012). Consistent with this idea, GmREM1.1 and GmREM1.3, which have similar RemCA peptides that share amphipathic α -helix properties with that of StREM1.3, were shown to require RemCA for PM targeting (Fig. 2-2A). In contrast, the GmREM2.1 RemCA region shared only 47% sequence identity with that of StREM1.3 and could not localize to the PM alone (Fig. 2-2B). Recently, RemCA in MtSYREM1, a group 2 remorin, was entirely associated with the PM even though there were remarkable sequence differences between the RemCA regions (Konrad et al., 2014). Therefore, the PM localization ability of RemCA must not be a special feature of group 1 remorins, and rather, overall sequence conservation or several unknown determinant residues might exist in the RemCA motif. Introducing point mutations in the RemCA motif will provide further insight into its exact roles in GmREM targeting.

GmREM1.1 and GmREM2.1 have distinct roles during root nodule

development

The expression patterns of *GmREM1.1* and *GmREM2.1* suggested that both group 1 and group 2 *GmREMs* participate in nodule developmental processes, possibly with distinct roles (Fig. 2-3). Although group 1b remorins generally showed increased expression in mature and/or senescing tissues (Bariola et al., 2004) and high, ubiquitous expression in *Arabidopsis* (Raffaele et al., 2007), the expression levels of *GmREMs* were differentially regulated during nodule maturation (data not shown). The spatiotemporal expression pattern of *GmREM1.1* and *GmREM2.1* showed that their major transcription sites were separated from each other in the developing nodules as inner cortex versus infected cells, providing relevant evidence for their discrete roles during nodule development (Fig. 2-3).

Generally, root nodule development is composed of two genetically separated processes, bacterial infection and nodule organogenesis (Oldroyd et al., 2011). Because *GmREM1.1* is primarily expressed at the nodule primordia and inner cortex regions where symbiotic microbes are rare, our results suggest that GmREM1.1 may be implicated in the nodule organogenesis process rather than bacterial infection. This hypothesis is further supported by the fact that its expression was dramatically decreased during nodule maturation (data not

shown). However, *GmREM2.1* transcripts were highly detected in the nodule infection zone and maintained at a constant level during nodule development. In addition, *GmREM2.1* transcription was also induced in *B. japonicum*-inoculated root hairs after 2 DAI by a global transcriptome analysis (Libault et al., 2010) and our preliminary experiment using *GmREM2.1::GUS* transgenic hairy roots (data not shown). This evidence suggests that *GmREM2.1* must be involved in the bacterial infection process and maintenance, such as metabolic exchanges during nodule development.

Because *GmREM2.1* seems to be a soybean orthologous gene for *MtSYREM1* and *LjSYREM1* based on sequence similarities and nodule-specific expression (Lefebvre et al., 2010; Toth et al., 2012), I examined the functional consistency by generating *RNAi-GmREM* hairy roots. In agreement with the *RNAi-MtSYREM1* nodules, silencing *GmREM2.1* resulted in a significant reduction in nodule formation (Fig. 2-4A). However, *RNAi-GmREM1.1* hairy roots produced a similar number of nodules in the control plants (Fig. 2-4A). This result may be attributed to the fact that at least eight members of group 1 remorin are present in the soybean genome, and these genes could perform their roles redundantly during nodule development. More delicate approaches, such as multiple gene silencing, overexpression, and genome-wide assays, will be

helpful to unravel how GmREM2.1 and GmREM1.1 respond and transduce the extracellular microbe signals to unknown downstream regulators. Furthermore, considering the previously proposed remorin roles as molecular scaffold proteins (Toth et al. 2012), a fascinating question is to investigate the type of protein complex that is assembled by GmREMs in membrane microdomains during legume-rhizobium symbiosis.

CHAPTER II.

Arabidopsis thaliana remorins
interact with SnRK1 and play a role in
susceptibility to beet curly top and beet
severe curly top viruses

3.1 Abstract

Remorins, a family of plant-specific proteins containing a variable N-terminal region and conserved C-terminal domain, play a role in various biotic and abiotic stresses, including host-microbe interactions. However, their functions remain to be completely elucidated, especially for the *Arabidopsis thaliana* remorin group 4 (AtREM4). To elucidate the role of remorins in *Arabidopsis*, I first showed that AtREM4s have typical molecular characteristics of the remorins, such as induction by various types of biotic and abiotic stress, localization in plasma membrane and homo- and hetero-oligomeric interaction. Next, I showed that their loss-of-function mutants displayed reduced susceptibility to geminiviruses BSCT and BSCTV, while overexpressors enhanced susceptibility. In addition, I found that they interacted with SnRK1, which phosphorylated AtREM4.1, and were degraded by the 26S proteasome pathway. Moreover, the co-expression of AtREM4.1 with transcription factor

AtTCP14 led to a BiFC signal in the nucleus. These results suggest that AtREM4s may be involved in the SnRK1-mediated signaling pathway and play a role as positive regulators of the cell cycle during geminivirus infection.

3.2 Introduction

Geminiviruses are approximately 2.8 kb single-stranded circular plant DNA viruses that can cause serious losses of crop products worldwide (Vanderschuren et al., 2007). They are divided into four genera: *Mastrevirus*, *Curtovirus*, *Topocuvirus*, and *Begomovirus*. *Beet curly top virus* (BCTV) and *Beet severe curly top virus* (BSCTV) are *Curtoviruses* that infect only phloem-limited dicotyledonous plants and raise symptoms such as stunted growth, leaf curling, accumulation of anthocyanin, vein swelling and hyperplasia of the phloem (Latham et al., 1997). Geminiviruses regulate several signaling pathways involved in cell cycle regulation and host defense for the purpose of viral propagation. Infection with geminiviruses leads to cell cycle reprogramming using RBR. Viral proteins such as AL1 (also known as AC1, C1 and Rep) and C3 (also known as REn) bind to RBR and inhibit it (Kong et al., 2000; Desvoyes et al., 2006); thus, the infected cells express genes associated with the onset of G1, S and early G2 phases, while suppressing those associated with the early G1 and late G2 phases (Ascencio-Ibanez et al., 2008).

Plants have innate antiviral defense systems such as gene silencing, and regulation of salicylic acid biosynthesis and metabolism (Zhang et al., 2011).

Geminiviruses also interfere with these defense systems. To facilitate geminivirus replication, C2 interacts with ADK and SAMDC1 and suppresses the plant methyl cycle (Wang et al., 2005; Zhang et al., 2011), and inhibits SnRK1 (Hao et al., 2003). SnRK1-mediated innate antiviral defense was identified by the interaction of geminivirus C2 proteins with SnRK1.2 (Hao et al., 2003), and it was reported that S1SnRK1 reduces geminivirus infection by interacting with and phosphorylating the β C1 protein (Shen et al., 2011). SnRK1 is a key regulator of plant stress and metabolism, and it regulates global transcription (Baena-Gonzalez et al., 2007). Therefore, it is suggested that SnRK1 may also control many levels of transcription during geminivirus infection; however, the antiviral signaling pathway of SnRK1 is largely unknown.

Geminiviruses also protect some unstable host proteins such as GRIK and SAMDC1 from degradation (Shen and Hanley-Bowdoin, 2006; Zhang et al., 2011) and utilize the ubiquitin pathway for viral replication (Alcaide-Loridan and Jupin, 2012). They hijack the ubiquitin ligase complexes that are key regulators of several processes, including the cell cycle, for modulating host function. The C2 protein changes several plant hormone responses using the CUL1-based SCF ubiquitin E3 ligases (Lozano-Duran et al., 2011), and C4

activates plant cell proliferation using RKP ligase that targets cyclin kinase inhibitors for proteasomal degradation (Lai et al., 2009). In addition, the Clink protein bound to RBR and SKP1 was supposed to alter ubiquitination to affect cell cycle regulation (Aronson et al., 2000). Indeed, during geminivirus infection, there was a general increase in the transcription of genes encoding components of the ubiquitin-proteasome pathway and ubiquitin enzymes (Ascencio-Ibanez et al., 2008).

Remorins are plant-specific proteins, first reported as plasma membrane (PM) proteins in leaves of tomatoes and potatoes phosphorylated in the presence of polygalacturonide (Farmer et al., 1989). Some of them have been found in detergent-insoluble membranes called lipid rafts (Mongrand et al., 2004; Laloi et al., 2007; Lefebvre et al., 2007). Remorins, found in all land plants, are a family of proteins comprised of six different groups (Raffaele et al., 2007). Remorin genes are expressed in diverse tissues, such as embryonic, shoot apex, and vascular tissues (Bariola et al., 2004), and are induced in dehiscent tissues, source parts of the leaves, and aging organs of tobacco (Raffaele et al., 2009a). Furthermore, mRNA and protein levels of some remorins are regulated by various abiotic stressors, hormones and pathogens (Coaker et al., 2004; Nohzadeh Malakshah et al., 2007; Raffaele et al., 2007;

Widjaja et al., 2009; Li et al., 2012a).

Remorin proteins have a variable N-terminal, a conserved C-terminal (Remorin_C; PF03763), and a Pfam domain. The N-terminal is responsible for structural and functional divergence, whereas the C-terminal, which includes the coiled-coil motif, is important for oligomerization and localization in the PM. Recently, it was shown that the 28-amino acid C-terminal of StREM1.3, the remorin C-terminal Anchor (RemCA), was necessary and sufficient for PM targeting (Perraki et al., 2012).

Studies on plant-virus and plant-microbe interactions have reported a variety of functions for remorin. Researchers have shown that Potato StREM1.3 binds cell wall-derived galacturonides (Reymond et al., 1996) and interacts with the viral protein TGBp1 of potato virus X (Raffaele et al., 2009b); REM1.3 remorin enhances susceptibility to *Phytophthora infestans* (Bozkurt et al., 2014); *Arabidopsis thaliana* remorin 1.3 (AtREM1.3) is differentially phosphorylated after treatment with a bacterial elicitor (Benschop et al., 2007; Jarsch and Ott, 2011) and AtREM1.2 has been identified as RIN4, a negative regulator of plant immunity. (Liu et al., 2009). In addition, MtREM2.2, phosphorylated by RLK, regulates bacterial infection (Lefebvre et al., 2010), and AtREM1.3 interacts with IMPa and translocates to the nucleus (Marin et al.,

2012). Although remorins have been expected to function as scaffold proteins in many important signaling pathways, their role in the signaling process is remains unknown.

Since there is little information on the remorins belonging to group 4, I studied *AtREM4.1* and *AtREM4.2* as the first step in understanding their biological functions in *Arabidopsis*. I found that they are highly regulated by osmotic stress and senescence, and they are positive regulators of geminivirus infection through interacting with SnRK1.

3.3 Materials and methods

3.3.1 Plant materials and virus inoculation

All *Arabidopsis* used in this study were of the Columbia (Col-0) ecotype. *AtREM4.1-1*, *AtREM4.2-1* and *AtREM4.2-2* mutants were obtained from the SALK (SALK_063269C, SALK_119462 and SALK_143766) and the double mutants were constructed by crossing *AtREM4.1* and *AtREM4.2* mutants. For the transgenic plants of *pAtREM4.1:GUS* and *pAtREM4.2:GUS*, the 1622 base pair (bp) upstream region of *AtREM4.1* and 1544 bp upstream region of *AtREM4.2* were amplified with primers (Table 3-2) by using genomic DNA. These were then cloned into the gateway pBGWFS7 vector. For overexpression lines, *AtREM4.1* and *AtREM4.2* were inserted into the pEarleyGate102 binary vector (Earley et al., 2006), then transgenic plants were generated using *Agrobacterium tumefaciens* GV3101 strains containing the constructs by a floral dip method (Zhang et al., 2006).

For virus inoculation, seeds were sowed in soil for 3 days at 4°C, and plants were grown under 100 $\mu\text{mol m}^{-2} \text{s}^{-1}$ white fluorescent lights with a 16 h light and 8 h dark cycle at 22°C. The *Agrobacterium* strains containing BCTV, BSCTV, and control vector pMON, were inoculated in the crown of the rosette

of four-week-old plants using a needle as previously described (Lee et al., 1994).

3.3.2 Sequence analyses

ClustalW2 (<http://www.ebi.ac.uk/Tools/msa/clustalw2/>) and Boxshade (http://www.ch.embnet.org/software/BOX_form.html) programs were used to align the amino acid sequences. Conserved motifs of the protein were identified using MEME (<http://meme.sdsc.edu/meme/intro.html>) and ELM (<http://elm.eu.org/>) programs. Coiled-coil motifs were predicted using Marcoil (<http://bioinf.wehi.edu.au/folders/mauro/Marcoil/index.html>). Putative phosphorylation site and PEST motifs were predicted using NetPhos 2.0 (<http://www.cbs.dtu.dk/services/NetPhos/>) and epestfind (<http://emboss.bioinformatics.nl/cgi-bin/emboss/epestfind>).

3.3.3 Gene expression analysis

For reverse transcription-polymerase chain reaction (RT-PCR), 2 µg of total RNA isolated from the plants using TRIzol (Invitrogen, USA) was used as a template for cDNA, and it was performed using the gene specific primers (Table 3-1). The *Actin-2* gene was used as a loading control for PCR. For

promoter activity analysis, the T3 transgenic plants of *pAtREM4.1:GUS* and *pAtREM4.2:GUS* were treated with MES, 100 µM ABA and 150 mM NaCl at 3 h. For histochemical analysis, plants were incubated at 37°C for 4 h in the GUS staining buffer (100 mM sodium phosphate (pH 7.0), 10 mM EDTA, 0.5 mM K₃[Fe(CN)₆], 0.5 mM K₄[Fe(CN)₆], 0.1% Triton X-100) supplemented with 0.5 mM X-Gluc. Chlorophyll was cleared as previously described (Jefferson et al., 1987).

3.3.4 Yeast two-hybrid assay

Full length cDNA, such *AtREM1.4*, *AtREM4.1*, *AtREM4.2* and *SnRK1.2*, and truncated cDNA, such as *AtREM4.1N* (amino acid 1-179), *AtREM4.1C* (amino acid 180-296), *AtREM4.2N* (amino acid 1-157) and *AtREM4.2C* (amino acid 158-275) were amplified with the primers (Table 3-2), and the amplified fragments were ligated into the pGAD GH and pGBT9 BS vectors. The constructs were concurrently transformed to the pJ69-4a yeast strain, and the double transformants in pJ69-4a strains were selected as cells grown in the absence of leucine and tryptophan. The selected double transformants were transferred and grown in the absence of adenosine, histidine, leucine, and tryptophan for interaction selection.

3.3.5 Bimolecular fluorescence complementation (BiFC) and localization of fluorescent conjugated proteins

AtREM1.4, *AtREM4.1*, *AtREM4.2*, *AtTCP14*, *dynein* (*At3g16120*) and *SnRK1.2* were amplified with the primers Table 3-2 and inserted into the pSPYNE173 and pSPYCE(MR) vectors (Waadt et al., 2008). The constructs were transformed to GV3101 and BiFC was performed as previously described (Voinnet et al., 2003). The GV3101 strains contained each construct at an OD₆₀₀ of 0.5 and were coinfiltrated with the p19 strain at an OD₆₀₀ of 0.3 into 4-week-old tobacco plants (*N. benthamiana*). Confocal imaging was performed 3-5 days after infiltration with the LSM700 confocal laser-scanning microscope (Carl Zeiss, Germany). To analyze the localization of AtREM4.1-CFP and AtREM4.2-CFP, I used 5-day-old seedlings of *Arabidopsis* overexpressing *AtREM4s*, and the confocal images were obtained from root.

3.3.6 Expression and purification of recombinant proteins

AtREM4.1, *AtREM4.2*, *GRIK1*, and truncated *SnRK1.2* (amino acid 1-342) were amplified with the primers listed in Table 3-2. PCR products were cloned into pGEX4T-1 and transformed into *Escherichia coli* strain BL21(DE3)pLysS.

Cells in log-phase growth were grown in the presence of 1 mM IPTG for 20 h at 20°C. Total protein was extracted using BugBuster (Novagen, USA) and purified using GST resin (ElpisBiotech, Korea).

3.3.7 *In vitro* kinase assay

In vitro kinase assay was performed as previously described (Shen et al., 2009). Recombinant proteins (250 nM) were incubated with reaction buffer (25 mM Tris-HCl, pH7.5, 10 mM MgCl₂, 1 mM EGTA, 1 mM DTT, 0.2 mM cold ATP, and 0.5 µCi/µL [γ -³²P]ATP) at 30°C for 1 h, and the reaction was stopped by 5× SDS-PAGE sample buffer. An equal volume of each sample was loaded and separated in 8% SDS-PAGE gels. After protein separation, the gels were lapped and ³²P-labeled proteins were visualized by autoradiography on X-ray films (Fujifilm, Japan).

3.3.8 Cell free degradation assay

Seedling powders of *Arabidopsis* that were ground in liquid nitrogen were resuspended in degradation buffer containing 25 mM Tris-HCl, pH 7.5, 10 mM NaCl, 10 mM MgCl₂, 5 mM DTT, 10 mM ATP and 4 mM PMSF and total proteins were extracted as previously described (Wang et al., 2009).

Recombinant AtREM4 proteins were incubated in equal quantities of extracts with DMSO or 40 μ M MG132 at 22°C for the indicated times, and the reaction was stop by 5 \times SDS-PAGE sample buffer. An equal volume of each sample was separated in 8% SDS-PAGE gel, and immunoblots were performed with GST antibody. The band quantifications of the remaining protein on immunoblots were measured using IMAGEJ (<http://rsb.info.nih.gov/ij/index.html>).

Table 3-1. Primers used for RT-PCR.

Gene	Purpose	Primers (5' → 3')	
AtREM1.4	RT-PCR	F	AGAGTTCAGAATCATTTGATT
		R	GAACGTCATTACATCAAATACCA
AtREM4.1	RT-PCR	F	CAGACCTAAACTAGCTAATTACA
		R	GGTAGCCTATATATATTGAGACA
AtREM4.2	RT-PCR	F	TAGACGATCACAAATTCTAAACC
		R	GTACATGAGCTATAAACTGCC
Actin-2	RT-PCR	F	ATGGCTGAGGCTGATGATATT
		R	AGAAACATTTCTGTGAACGATT
RD29A	RT-PCR	F	TGGATCTGAAGAACGAATCTGATATC
		R	GGTCTCCCTTCGCCAGAA
ATHB12	RT-PCR	F	GGTTAGACCAAGGGAGTGTCTATGT
		R	CAATTCTCAGAAGATGTCAAGCACT
RKP	RT-PCR	F	TTCGTAGTTACACACTTCAAC
		R	TCATGTGCTCTTTGTGACC
PR5	RT-PCR	F	AGCCTCGTAGATGGTTACAATGTC
		R	GGTTTTAAGGGCAGAAAGTGATT
PDF1.2	RT-PCR	F	TCATGGCTAAGTTGCTCC
		R	AATACACACGATTAGCACC

Table 3-2. Primers used for constructs.

Gene	Purpose	Primers (5' → 3')	
AtREM4.1 P	Promoter	F	GC GGCC GCGGAGGTATATGTGTTG
		R	GG CGCG CCTCTTGACCGTACAAAGTC
AtREM4.2 P	Promoter	F	GC GGCC GCTTGACAGCTCTAAATGTG
		R	GG CGCG CCCTTGATGGTAAAGAGTCA
AtREM4.1 OX	Overexpression	F	CACCATGTTGACTTTGTACGGTCAA
		R	GGAAAGAGAGAAGAACATCGTTGG
AtREM4.2 OX	Overexpression	F	CACCATGCTGACTCTTACCATC
		R	GGAGAAAGAGAAGAACGGAGC
AtREM1.4	Y2H	F	ACTAGT GATGGCTGAAGAGGAACCG
		R	GTCGACTCACATGCATCCGAAAAG
AtREM4.1	Y2H	F	ACTAGT GATGTTGACTTTGTACGGT
		R	GTCGACCTAGGAAAGAGAGAAGAAT
AtREM4.2	Y2H	F	ACTAGT GATGCTGACTCTTACCATC
		R	CCCGGGTTATCTTGCACCGTCGAC
AtREM4.1N	Y2H	F	ACTAGT GATGTTGACTTTGTACGGT
		R	GTCGACCCTCTGCACCGAAG
AtREM4.1c	Y2H	F	ACTAGT GATG GTGAAGAGAGAAGA
		R	GTCGACCTAGGAAAGAGAGAAGAAT
AtREM4.2N	Y2H	F	ACTAGT GATGCTGACTCTTACCATC
		R	CCCGGGTCTTGCACCGTCGA
AtREM4.2c	Y2H	F	ACTAGT GATGGTTAAGAGGGAAAGAG
		R	CCCGGGTTATCTTGCACCGTCGAC
SnRK1.2	Y2H	F	ACTAGT GATGGATCATT CATCAAATAG
		R	GTCGACTCAGATCACACGAAGCTCT
AtREM1.4	BiFC	F	ACTAGT ATGGCTGAAGAGGAACCG
		R	GTCGACCATGCATCCGAAAAG
AtREM4.1	BiFC	F	ACTAGT ATGTTGACTTTGTACGGT
		R	GTCGACGGAAAGAGAGAAGAATG
AtREM4.2	BiFC	F	ACTAGT ATGCTGACTCTTACCATC
		R	CTCGAGTCTTGCACCGTCGAC

AtTCP14	BiFC	F	GGATCCATGCAAAAGCCAACATC
		R	CTCGAGATCTTGCTGATCCTCCTC
Dynein	BiFC	F	ACTAGTATGTTGAAAGGAAAGCG
		R	GTCGACAAGAGTGGCGCCTTG
SnRK1.2	BiFC	F	ACTAGTATGGATCATTGATCAAATAG
		R	GTCGACGATCACACGAAGCTCT
AtREM4.1	Protein	F	GGATCCATGTTGACTTTGTACGGT
		R	CTCGAGCTAGGAAAGAGAGAAGAA
AtREM4.2	Protein	F	GAATTCATGCTGACTCTTACCATCA
		R	CTCGAGTTAGGAGAAAGAGAAGAAG
GRIK1	Protein	F	GAATTCATGTTTGTGATAGTTT
		R	CTCGAGTCAGCTATGGTTTGATC
SnRK1.2	Protein	F	GGATCCATGGATCATTGATCAAATAG
		R	CTCGAGTCAATAGCCACTTGGAACA

3.4 Results

3.4.1 Transcription of *AtREM4s* is highly enhanced by osmotic stress, abscisic acid and senescence

There are 16 remorin genes in *A. thaliana* and they are expected to be involved in various biotic and abiotic signaling pathways. However, their function is not known yet. To elucidate the role of remorin, I examined the expression levels of 16 remorin genes of *Arabidopsis* using the Genevestigator program (<https://www.genevestigator.com/gv/>) (data not shown). Interestingly, *AtREM4.1* and *AtREM4.2* were highly regulated by various osmotic stressors, ABA, high light, and pathogens. They have similar sequences and are likely to be recent duplicates of each other (Raffaele et al., 2007). Deduced AtREM4 proteins have proline and serine-rich N-terminal regions and each have the 89% conserved remorin C-terminal domain, a typical remorin protein structure (Fig. 3-1A). To validate the expression levels of *AtREM4s*, I performed RT-PCR using gene specific primers in various osmotic and ABA conditions. Indeed, their expressions were highly enhanced by mannitol, NaCl, drought, and ABA conditions (Fig. 3-1B). Moreover, their promoters were also activated strongly by NaCl and ABA (Fig. 3-1C). These two genes were predominantly detected in

bud, stem, root, flower, siliques, and leaves, and enhanced dramatically in senescence leaf (Fig. 3-1D).

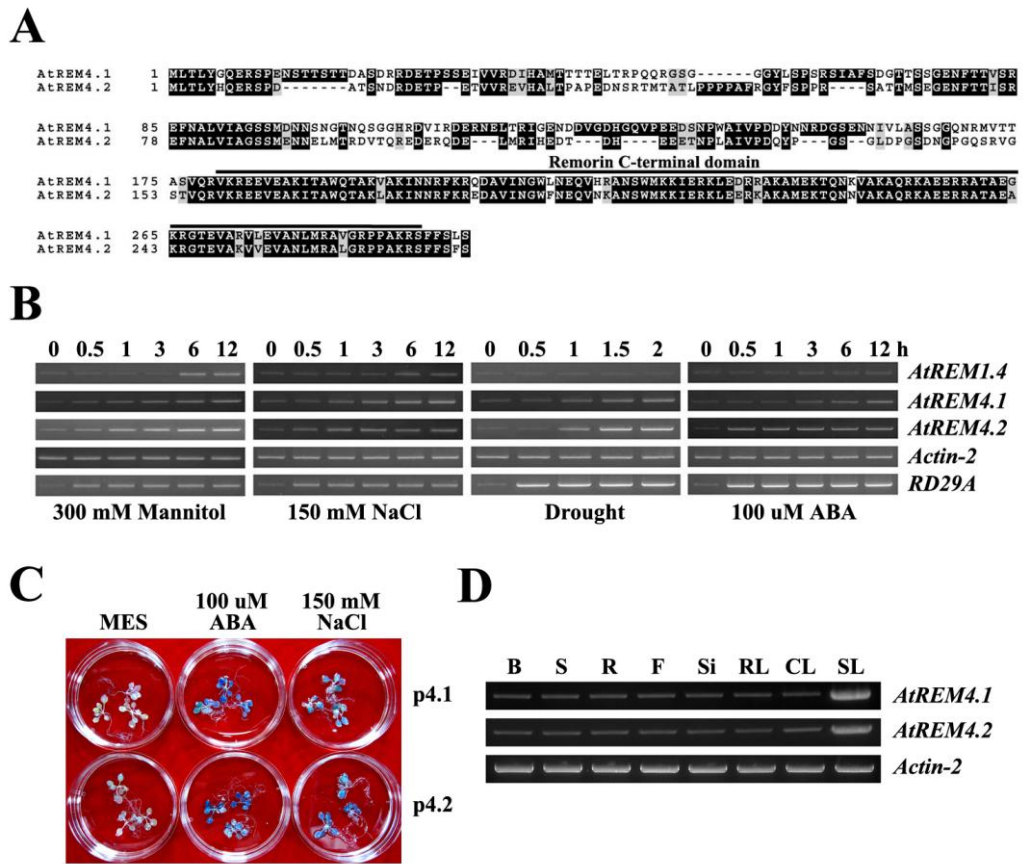


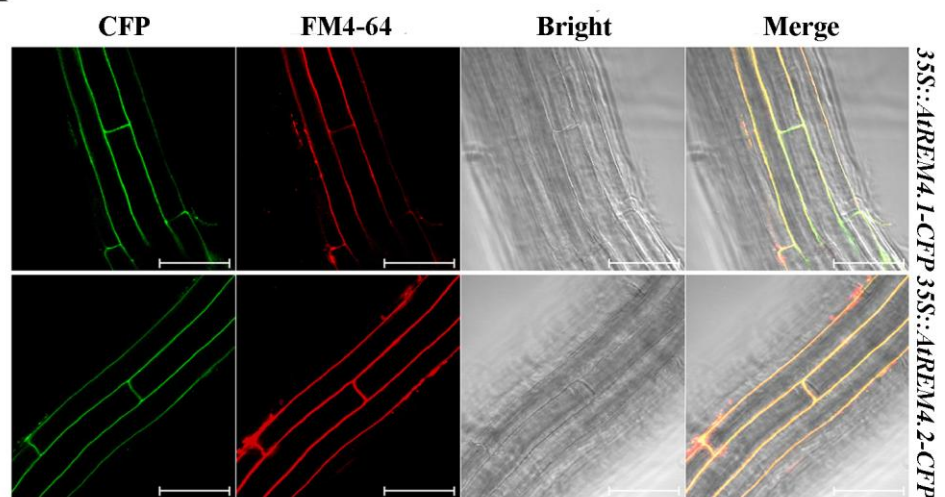
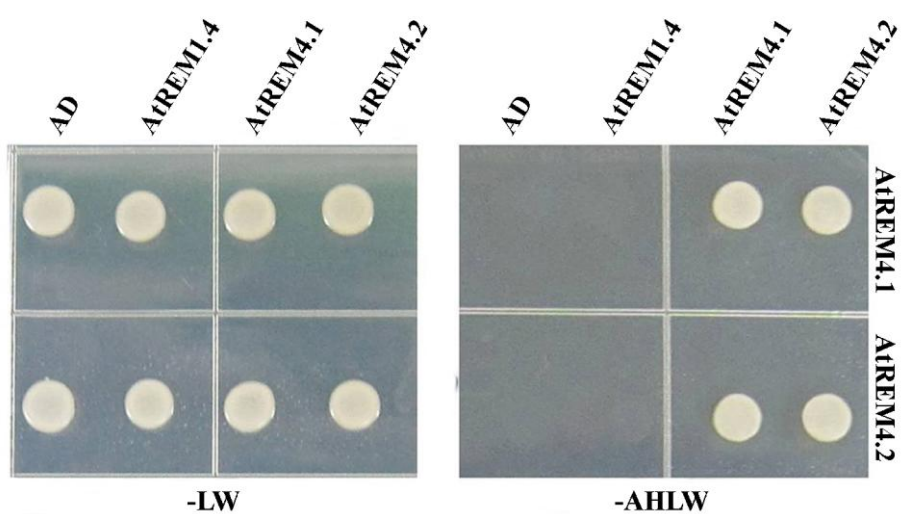
Figure 3-1. Amino acid alignment and expression level of *AtREM4s*. (A)

The amino acids sequence alignment of AtREM4s were constructed using the ClustalW software. Black boxes represent conserved amino acids and remorin C-terminal domains that were predicted by the Marcoil software. (B) RT-PCR was performed for stress responses using 2-week-old plants treated with 300 mM mannitol, 150 mM NaCl, drought and 100 μ M ABA at indicated time.

Actin-2 is used for a loading control and *RD29A* as a stress marker. (C) Promoter activity for stress response analysis. T3 transgenic plants were treated with MES, 100 µM ABA and 150 mM NaCl at 3 h, and then GUS-staining was performed. The 1622-bp upstream region of *AtREM4.1* is indicated by p4.1, and p4.2 represents the 1544-bp upstream region of *AtREM4.2*. (D) RT-PCR analysis for various tissues. *Actin-2* was used for loading control. B, bud; S, stem; R, root; F, flower; Si, siliques; RL, rosette leaf; CL, cauline leaf; SL, senescence leaf.

3.4.2 AtREM4 proteins form homo- and hetero-interactions in the plasma membrane

Remorin proteins are reported to localize in the PM, but localization of group 4 remorin proteins remain unknown. Therefore, in order to analyze the localization of AtREM4s in *Arabidopsis*, I used 35S::AtREM4-CFP transgenic plants. As a result, I could show that AtREM4s also targeted the PM (Fig. 3-2A). The remorin C-terminal domain, including the coiled-coil motif, was reported to mediate homo-interactions (Toth et al., 2012). Thus, I tested whether AtREM4 proteins that have similar amino acid sequences can interact with each other. In the yeast-two hybrid system, AtREM4s formed homo- and hetero-interactions. However, they did not interact with group 1 remorin protein AtREM1.4 (Fig. 3-2B). To confirm this result *in planta*, I performed BiFC using *N. benthamiana* leaves, where strong interactions of AtREM4s were observed in the PM of infiltrated tobacco epidermal cells (Fig. 3-2C).

A**B**

C

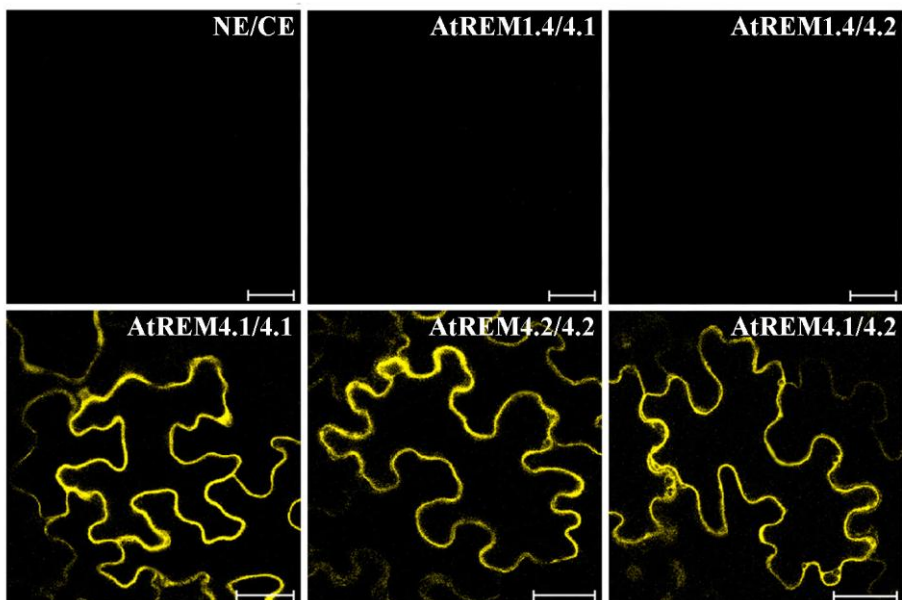


Figure 3-2. Subcellular localization and oligomeric interactions of AtREM4s. (A) Confocal images of $35S::AtREM4.1-CFP$ and $35S::AtREM4.2-CFP$ in 5-day-old seedlings. FM4-64 was used for PM staining marker. Bars = 50 μ m. (B) Y2H analysis for interaction among AtREM1.4, AtREM4.1 and AtREM4.2. (C) BiFC analysis of homo- and hetero-oligomeric interactions between AtREM4s in *N. benthamiana*, as described in the Materials and Methods. The fluorescence indicates the interaction between the indicated

partner proteins. BiFC cloning vectors, NE and CE, and AtREM1.4 were used as control. Scale bar = 50 μ m.

3.4.3 Double mutants of *AtREM4s* reduce the BCTV and BSCTV susceptibility

To study the function of *AtREM4s*, I generated double mutants (Fig. 3-3A) and overexpression lines (data not shown) to test their involvement in plant-microbe interaction. Interestingly, *AtREM4* double mutants showed reduced BCTV and BSCTV susceptibility (Fig. 3-3B). To confirm this, I inoculated the *Agrobacterium* that contained the BSCTV genome to *AtREM4* mutant and overexpression lines. As a result, single mutants showed slightly reduced susceptibility, whereas overexpression lines showed severe stunting of growth, severe curling of leaves and malformed inflorescence structures (Fig. 3-3C). Based on severity of infection rates, classified as previously described (Park et al., 2011), the difference was more evident (Fig. 3-3D). At 3 weeks after BSCTV inoculation, approximately 75% of wild-type (WT) plants developed severe symptoms. However only 10% of the plant double mutants showed severe symptoms, while more than 80% of the overexpression lines showed severe infection. Next, RT-PCR was performed to examine the infectivity at molecular level. It was reported that *ATHB12* and *RKP* were induced by BSCTV C4 (Lai et al., 2009; Park et al., 2011). Thus, I used *ATHB12* and *RKP* as marker genes of BSCTC susceptibility. *ATHB12* and *RKP* were expressed

highly in WT and overexpression lines, but slightly in double mutants (Fig. 3-3E). The gene profiling data showed that markers of SA response such as *PR1* and *PR5* were elevated during geminivirus infection, while transcripts for some JA markers such as *PDF1.2* were reduced (Ascencio-Ibanez et al., 2008; Yang et al., 2008). Indeed, *PR5* was increased more in WT and overexpression lines than mutant lines, whereas *PDF1.2* higher in mutant lines than WT and overexpression lines (Fig. 3-3E). These results indicate that AtREM4 regulate positively the BCTV and BSCTV susceptibility.

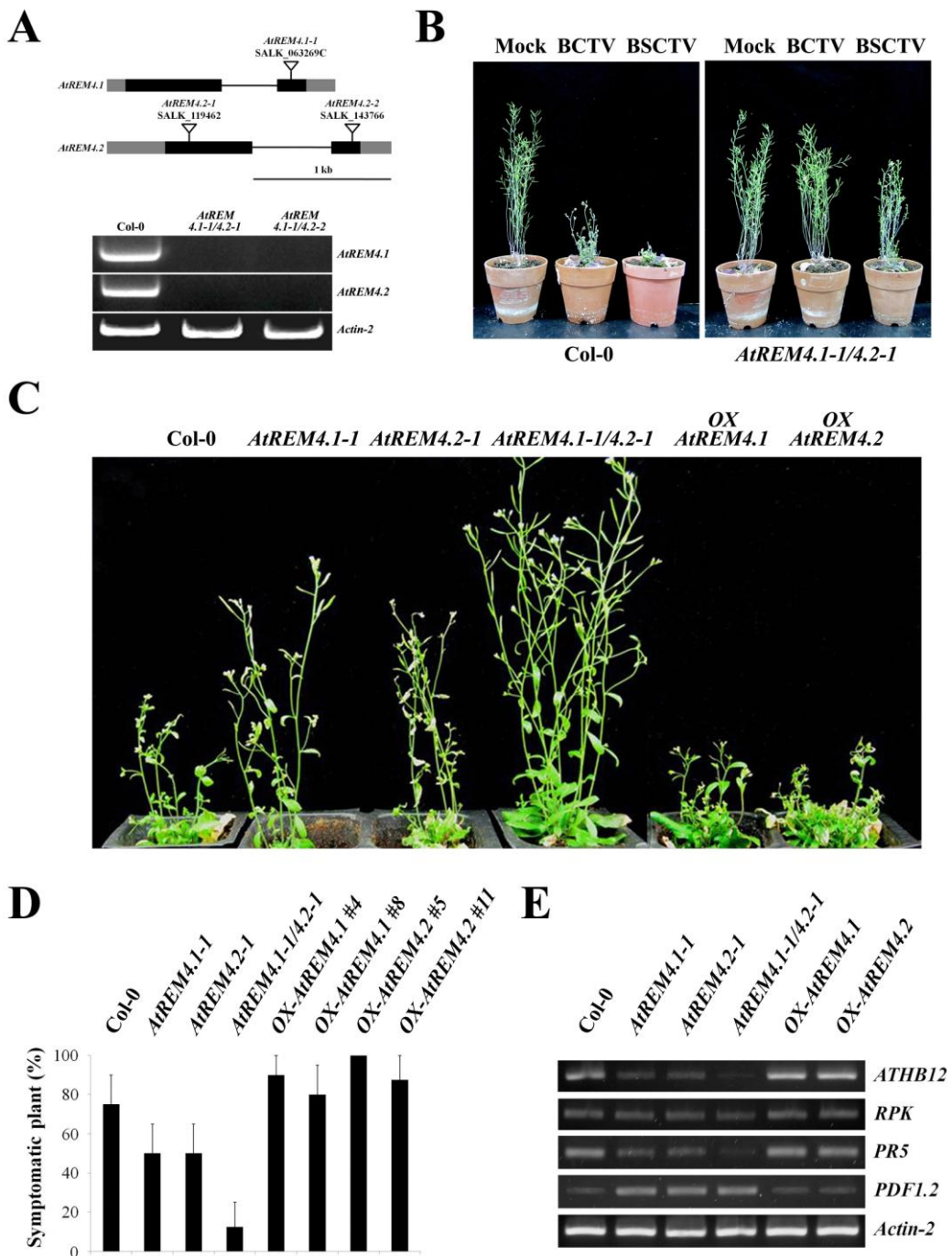
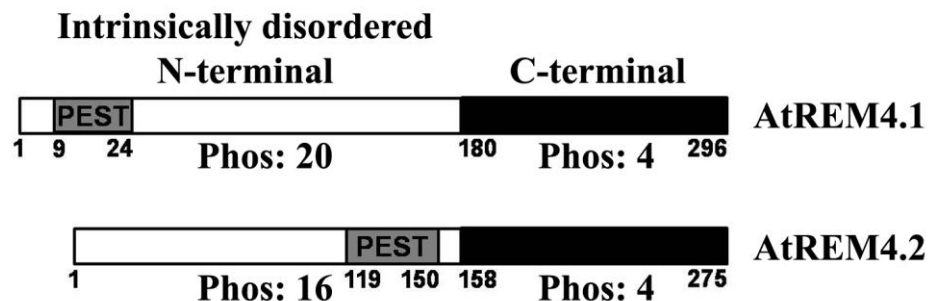
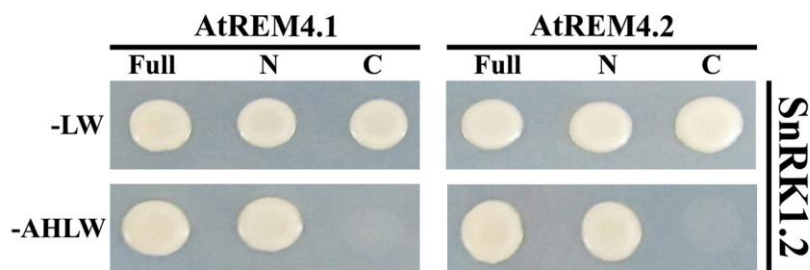
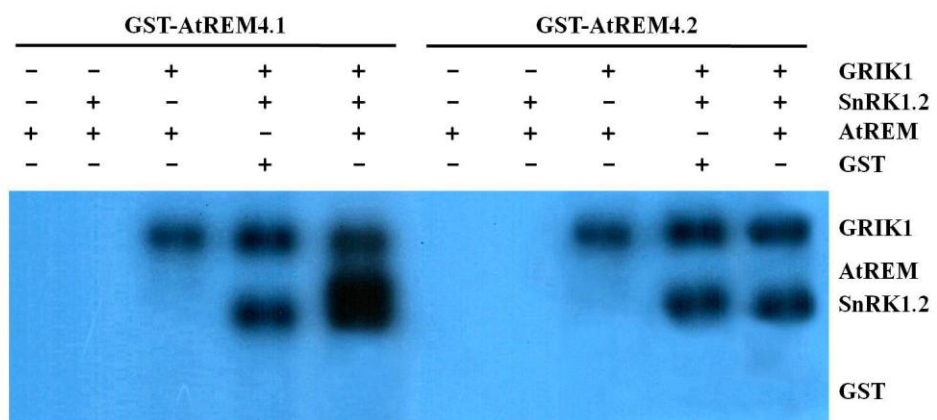


Figure 3-3. Geminivirus susceptibility of *AtREM4s*. (A) The gene structures and T-DNA insertion sites. Black boxes are exons, and gray boxes are untranslated regions. Intergenic regions or introns are marked with lines. Expression levels of *AtREM4s* in the double mutants as assayed by RT-PCR. (B) For the geminivirus infection experiment, *Agrobacterium* stains containing BCTV, BSCTV and control vector, pMON, were inoculated in the crown of the rosette of four-week-old WT and double mutant plants using a needle. (C) BSCTV infection experiments were performed using WT, *AtREM4.1-1*, *AtREM4.2-1*, *AtREM4.1-1/4.2-1*, 35S::*AtREM4.1-CFP* and 35S::*AtREM4.2-CFP*. (D) For severely infected plants, plant symptom severity rates were classified as previously described (Park et al., 2011). (E) For RT-PCR, total RNA was isolated from the plants that were infected with BSCTV, and RT-PCR was performed. The *Actin-2* gene was used as a loading control for PCR.

3.4.4 AtREM4s interact with SnRK1.2 and AtREM4.1 is phosphorylated by it. Using computer software, electrophoretic mobility, and heat stability, I found that AtREM4s have intrinsically disordered N-terminal regions (data not shown). They are flexible and modified by several different enzymes such as kinases, ubiquitin-ligases, acetyltransferases and methylases (Dyson and Wright, 2005). Indeed, a bioinformatic analysis of AtREM4s predicted putative phosphorylation sites and PEST motifs within the N-terminal regions (Fig. 3-4A). Using Y2H library screening, I identified AtREM4-interacting protein partners including SnRK1.2 and ubiquitin-proteasome components (data not shown). AtREM4s has many serines and threonines in the N-terminal region, and the phosphorylation prediction program NetPhos2 predicted more than 20 amino acids to be phosphorylated (Fig. 3-4A). Thus, I examined which regions mediated this interaction using truncated versions of the gene. N-terminals of AtREM4s interacted with SnRK1.2, but C-terminals did not (Fig. 3-4B). To address whether AtREM4s are phosphorylated by SnRK1.2, I performed in vitro kinase assays using recombinant proteins with GRIK1, an upregulator of SnRK1 (Hao et al., 2003; Shen et al., 2011). Various combinations of recombinant AtREM4s, SnRK1.2 and GRIK1 proteins were incubated in the presence of [γ -³²P]ATP, and phosphorylation was visualized by autoradiogram-

phy. The signal band was detected strongly in the GST-AtREM4.1 loading line, but not in the GST-AtREM4.2 line (Fig. 3-4C). Quantitative analysis of the signal intensity rate also showed that only GST-AtREM4.1 shows an intense signal (Fig. 3-4D).

A**B****C**

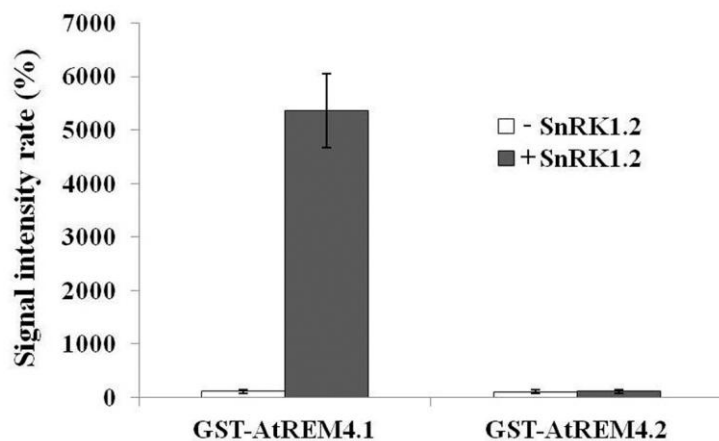
D

Figure 3-4. Phosphorylation of AtREM4s by SnRK1.2 *in vitro*. (A)

Schematic representation of AtREM4 domains. Putative PEST domain and phosphorylation site numbers are shown. Numbers indicate amino acid positions. (B) Y2H analysis to determine interacting domains of AtREM4s with SnRK1. Constructs of full length and truncated N and C-terminal ends of AtREM4s were used. (C) In vitro kinase assay for recombinant proteins of AtREM4s, SnRK1.2 and GRIK1. The reactions were resolved by SDS-PAGE gel and visualized by autoradiography. (D) Quantification analysis for the band signal intensity was measured by ImageJ, and the signal intensity rates were calculated such as (GST-AtREM4 intensity/GST intensity) × 100.

3.4.5 AtREM4s are degraded by the 26S proteasome pathway. Many unstable proteins that are degraded by the 26S proteasome have a PEST motif (Rogers et al., 1986; Rechsteiner and Rogers, 1996). Thus, I tested whether AtREM4 proteins are degraded in a proteasome-dependent manner. In the mock, GST-tagged AtREM4s were degraded rapidly, whereas the proteasome inhibitor MG132 apparently delayed the degradation such that with MG132 (Fig. 3-5A), GST-tagged AtREM4s remained 42-46% after 2 h, however, in mock, it remained only 5-10% (Fig. 3-5B). These results indicated that AtREM4s are degraded by the 26S proteasome-mediated signaling pathway.

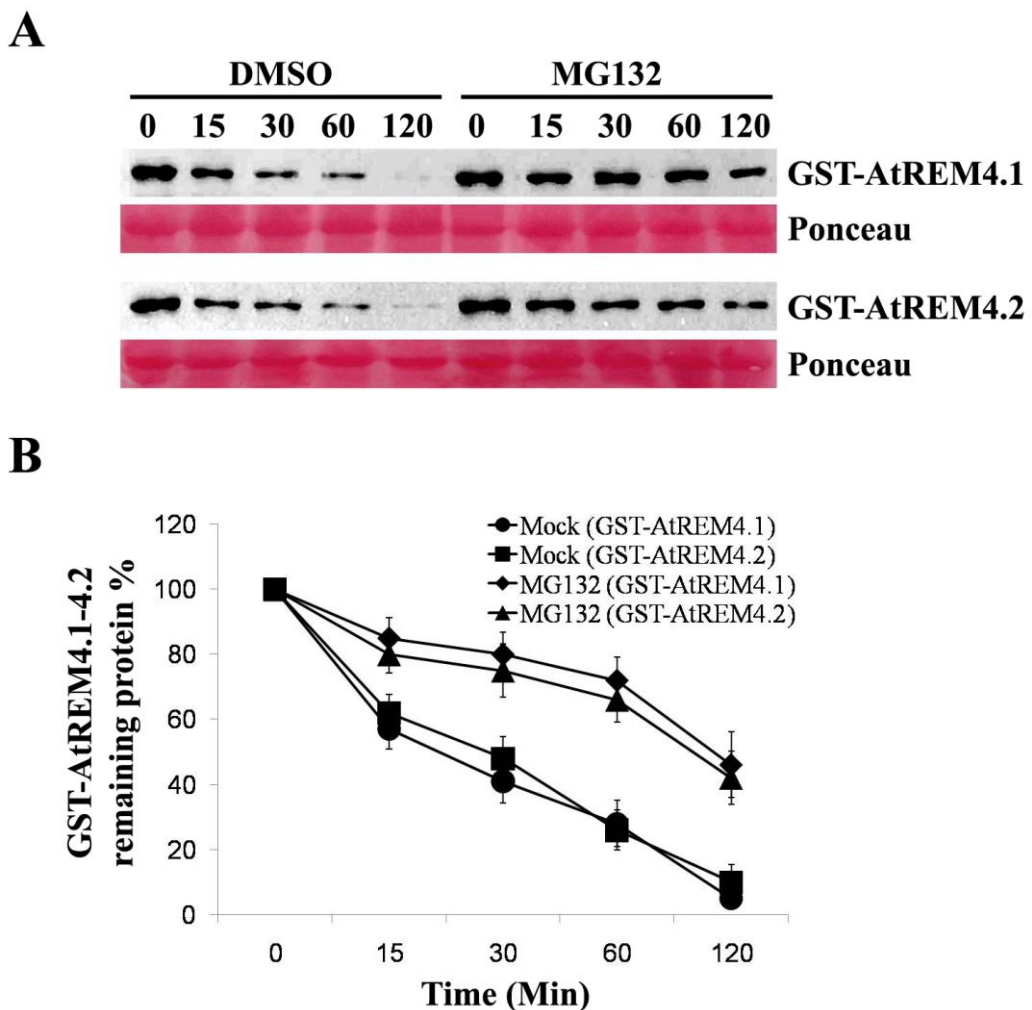


Figure 3-5. Cell free degradation of recombinant AtREM4 proteins. (A)

Immunoblot analysis for GST-AtREM4s degradation in the presence or absence of the proteasome inhibitor MG132. Recombinant GST-fusion proteins were expressed and purified from *E. coli* and then added to the total proteins that

were extracted from Col-0 for the indicated times. Immunoblots were probed with anti-GST antibody. Ponceau stain is shown as a loading control. (B) Quantification of the immunoblot analysis was performed using ImageJ.

3.4.6 Protein interactions leading to subcellular AtREM4.1 redistribution.

Previously, it was reported that AtTCP14 and dynein interact with AtREM4.1 in Y2H by *Arabidopsis* interactome mapping. Thus, I tested whether AtREM4.1 interacts with AtTCP14, dynein, or SnRK1.2 *in planta* in BiFC experiments, using constructs in different combinations in *N. benthamiana* leaves. Initially, I determined the subcellular localization of AtREM4.1 in tobacco leaves. AtREM4.1 fluorescence was detected in the PM (Fig. 3-6A). In addition, the BiFC signal resulting from AtREM4.1 homo-oligomerization was detected in the PM (Fig. 3-2C). However, coexpression of protein interaction partners such as AtTCP14, dynein, and SnRK1.2 altered the subcellular distribution of AtREM4.1. AtREM4.1 was almost exclusively localized to the nucleus when transcription factor AtTCP14 was coexpressed (Fig. 3-6B), whereas dynein coexpression resulted in BiFC signaling in the plasma membrane periphery and the cytosol (Fig. 3-6C). Interestingly, SnRK1.2 coexpression resulted in AtREM4.1 localization to the PM and cytosol in guard cells (Fig. 3-6D). Fluorescence signaling in guard cells was detected only in tobacco leaves that coexpressed SnRK1.2. These results indicate that AtREM4.1 interacts with AtTCP14, dynein, and SnRK1.2 *in planta* and that PM-associated remorins can

be translocated to various destinations, including the nucleus, cytosol, and guard cells by their interactive partners.

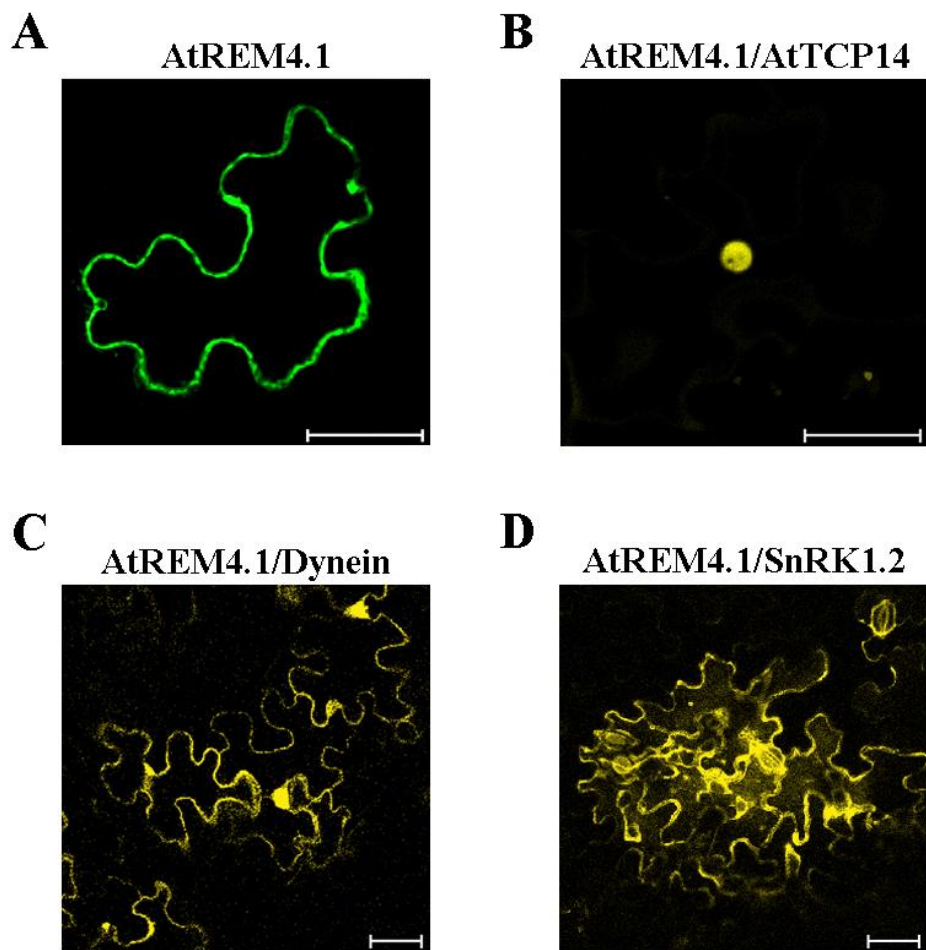


Figure 3-6. AtREM4.1 protein-protein interactions and cellular translocations *in planta*. For AtREM4.1 localization studies, tobacco leaves were infiltrated with an AtREM4.1 fluorescence construct (A). Using BiFC, AtREM4.1 protein interactions and translocation in *N. benthamiana* leaf epidermal cells were assessed with AtTCP14 (B), dynein light chain (C) and

SnRK1.2 (D). Confocal imaging was performed 3–5 days after infiltration using an LSM700 confocal laser-scanning microscope. Scale bar = 50 μ m.

3.5 Discussion

In this study, I present for the first time, the molecular characteristics of AtREM4s and their putative roles during the geminivirus infection process.

AtREM4s are typical remorins and their expression is highly stimulated by osmotic stress and senescence.

To date, most of the studies on remorins have focused on group 1 and 2. Thus, in this study, as the first step in elucidating the biological function of remorin group 4, I studied *AtREM4.1* and *AtREM4.2*. They showed typical characteristics of the remorin molecules, which consist of variable N-terminal and conserved C-terminal regions such as the remorin group 1 proteins (Fig. 3-1A). Remorins have been known to respond to various stress or developmental conditions. Transcription rates and protein levels of some group 1 remorins were regulated by salt, drought and ABA (Nohzadeh Malakshah et al., 2007; Raffaele et al., 2007), and the transcription of *NtREM1.2* increased with organ aging (Raffaele et al., 2009a). *AtREM4s* were also regulated similarly by abiotic and biotic stressors. However, of the 16 AtREMs, the expression of *AtREM4s* were induced to the greatest extent by various osmotic stressors and ABA (Fig.

3-1B). They were also expressed strongly in senescing leaves (Fig. 3-1D). Moreover, AtREM4s were localized in PM (Fig. 3-2A) and formed homo-oligomers (Fig. 3-2B) such as StREM1.3, AtREM1.3 and MtREM2.2. Interestingly, AtREM4s also formed hetero-oligomers, while did not with AtREM1.4 (Fig 3-2B), suggesting that they could share interacting components each other, and play redundant roles in the same signaling pathway.

AtREM4s enhance susceptibility to geminivirus by mediating SnRK1 and RBR interaction

In this study, I show that AtREM4s enhance susceptibility to geminivirus: overexpressors showed severe infection, while double mutants showed resistance (Fig. 3-3B). Interestingly, AtREM4s have putative motifs such as the FHA, BRCT and WW domains found in regulating complexes of cell division and DNA damage repair proteins. Geminivirus infection leads to cell cycle reprogramming of host plants and activation of G1/S transitioning for geminivirus DNA replication. RBR is a key negative regulator of that transition in plant cells (Gutzat et al., 2012). It binds and inactivates E2F transcription factors required for the expression of genes such as the host replication initiator proteins (Rep). Indeed, interaction of Rep with RBR led to the development of

geminivirus symptoms (Kong et al., 2000). Moreover, I show that AtREM4.1 was phosphorylated by SnRK1.2 *in vitro* (Fig. 3-4C) and that nuclear translocation of AtREM4.1 was mediated by TCP14 (Fig. 3-6B). SnRK1, a key regulator of plant stress and metabolism, is involved in plant antiviral defenses. However, the GRIK–SnRK1 cascade may become activated by infection to ensure that adequate energy and nutrient supplies are present to support viral and host DNA replication (Hanley-Bowdoin et al., 2013). AtTCP14 regulates the expression of several cell cycle-associated genes (including *RBR*) and binds directly to the *RBR* promoter at TCP-binding sites to activate its transcription (Li et al., 2012c). Functional analysis revealed that SnRK1 may collaborate with TCP transcription factors during stress and energy responses (Confraria et al., 2013). Moreover, during geminivirus infection, subsets of *Arabidopsis* TCPs are phosphorylated following activation of the GRIK-SnRK1 kinase cascade (Hanley-Bowdoin, unpublished). These results suggest that AtREM4s may be one of the intermediate regulators between SnRK1 and AtTCP transcription factor during geminivirus infection. Alternatively, they might be involved in a SnRK1-mediated defense-signaling pathway. To prove this hypothesis, I am in the process of elucidating the functional roles of AtREM4 and AtREM4-interacting partners using genetic and cell-biological approaches.

In addition, AtREM4s interacted with some ubiquitin-proteasome components (data not shown) and AtREM4.1 was degraded by the 26S proteasome (Fig. 3-5A). Previously, there were some reports that remorin protein levels were increased, while the expression was not changed or even decreased (Nohzadeh Malakshah et al., 2007; Widjaja et al., 2009). When I searched the PEST motifs, known as a signal for protein degradation, among 16 remorin proteins in *Arabidopsis*, they were predicted in N-terminals of 14 remorins except AtREM3.1 and AtREM3.2 (data not shown). These results suggest that decreased protein levels of the remorins mediated by the 26S proteasome, such as degradation of AtREM4 or AtREM4-interacting protein during the geminivirus infection process, might also be an important mechanism in regulating remorin-mediated signaling processes.

A model for the role of AtREM4s in regulating cell cycle progression and plant stress

Based on these results, a model was developed whereby the SnRK1-TCP and/or TCP-RBR-E2F signaling pathways may be linked by AtREM4s, thereby regulating the expression of cell cycle-associated and stress response genes (Fig 3-7). According to this model, GRIK activates SnRK1 during geminivirus

infection, which then phosphorylates AtREM4. Subsequently, AtREM4-TCP complexes translocate to the nucleus and it active cell cycle through the RBR-E2F signaling pathway. This model may also explain how geminiviruses exploit host factors to replicate the viral DNA. In cell lines encoding mutant *AtREM4* genes, the host plant cell cycle is not activated by geminiviral infection. Thus, geminiviruses do not replicate in these cell lines, resulting in decreased geminivirus susceptibility.

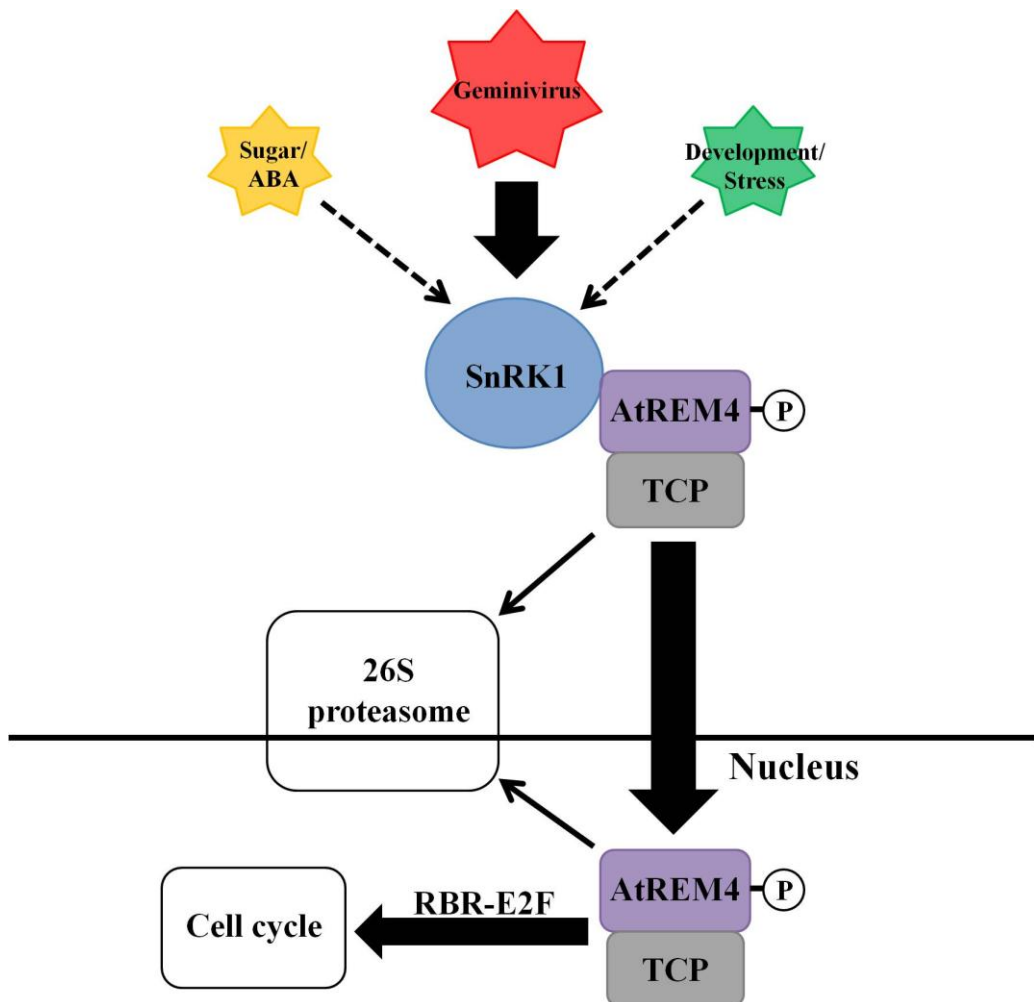


Figure 3-7. Proposed model for how AtREM4s may regulate cell cycle progression during geminivirus infection. The SnRK1-TCP-RBR-E2F signaling pathway is initiated by the interaction of AtREM4 with SnRK1 and transcription factor TCP. Subsequently, the AtREM-TCP complex translocates to the nucleus and regulates the expression of cell cycle-associated genes. Thick

arrows indicate a signaling pathway involving AtREM4s. Dotted arrows indicate pathways involving SnRK1, but AtREM4s are elusive. Thin arrows indicate AtREM4s degradation pathways.

REFERENCES

- Alcaide-Loridan, C., and Jupin, I.** (2012). Ubiquitin and plant viruses, let's play together! *Plant physiology* **160**, 72-82.
- Aronson, M.N., Meyer, A.D., Gyorgyey, J., Katul, L., Vetten, H.J., Gronenborn, B., and Timchenko, T.** (2000). Clink, a nanovirus-encoded protein, binds both pRB and SKP1. *Journal of virology* **74**, 2967-2972.
- Ascencio-Ibanez, J.T., Sozzani, R., Lee, T.J., Chu, T.M., Wolfinger, R.D., Cella, R., and Hanley-Bowdoin, L.** (2008). Global analysis of *Arabidopsis* gene expression uncovers a complex array of changes impacting pathogen response and cell cycle during geminivirus infection. *Plant physiology* **148**, 436-454.
- Baena-Gonzalez, E., Rolland, F., Thevelein, J.M., and Sheen, J.** (2007). A central integrator of transcription networks in plant stress and energy signalling. *Nature* **448**, 938-942.
- Bariola, P.A., Retelska, D., Stasiak, A., Kammerer, R.A., Fleming, A., Hijri, M., Frank, S., and Farmer, E.E.** (2004). Remorins form a novel family of coiled coil-forming oligomeric and filamentous proteins associated with apical, vascular and embryonic tissues in plants. *Plant molecular biology* **55**, 579-594.
- Benschop, J.J., Mohammed, S., O'Flaherty, M., Heck, A.J., Slijper, M., and Menke, F.L.** (2007). Quantitative phosphoproteomics of early elicitor

signaling in Arabidopsis. Molecular & cellular proteomics : MCP **6**, 1198-1214.

Bhat, R.A., Miklis, M., Schmelzer, E., Schulze-Lefert, P., and Panstruga, R. (2005). Recruitment and interaction dynamics of plant penetration resistance components in a plasma membrane microdomain. Proceedings of the National Academy of Sciences of the United States of America **102**, 3135-3140.

Boutte, Y., and Moreau, P. (2014). Plasma membrane partitioning: from macro-domains to new views on plasmodesmata. Frontiers in plant science **5**, 128.

Bozkurt, T.O., Richardson, A., Dagdas, Y.F., Mongrand, S., Kamoun, S., and Raffaele, S. (2014). The Plant Membrane-Associated REMORIN1.3 Accumulates in Discrete Perihaustral Domains and Enhances Susceptibility to Phytophthora infestans. Plant physiology **165**, 1005-1018.

Buday, L., and Tompa, P. (2010). Functional classification of scaffold proteins and related molecules. The FEBS journal **277**, 4348-4355.

Burack, W.R., and Shaw, A.S. (2000). Signal transduction: hanging on a scaffold. Curr Opin Cell Biol **12**, 211-216.

Checker, V.G., and Khurana, P. (2013). Molecular and functional characterization of mulberry EST encoding remorin (MiREM) involved in abiotic stress. Plant cell reports **32**, 1729-1741.

Coaker, G.L., Willard, B., Kinter, M., Stockinger, E.J., and Francis, D.M.

(2004). Proteomic analysis of resistance mediated by Rcm 2.0 and Rcm 5.1, two loci controlling resistance to bacterial canker of tomato. Molecular plant-microbe interactions : MPMI **17**, 1019-1028.

Collier, R., and Tegeder, M. (2012). Soybean ureide transporters play a critical role in nodule development, function and nitrogen export. The Plant journal : for cell and molecular biology **72**, 355-367.

Collier, R., Fuchs, B., Walter, N., Kevin Lutke, W., and Taylor, C.G. (2005). Ex vitro composite plants: an inexpensive, rapid method for root biology. The Plant journal : for cell and molecular biology **43**, 449-457.

Confraria, A., Martinho, C., Elias, A., Rubio-Somoza, I., and Baena-Gonzalez, E. (2013). miRNAs mediate SnRK1-dependent energy signaling in Arabidopsis. Frontiers in plant science **4**, 197.

Cortese, M.S., Uversky, V.N., and Dunker, A.K. (2008). Intrinsic disorder in scaffold proteins: getting more from less. Progress in biophysics and molecular biology **98**, 85-106.

Demir, F., Hornrich, C., Blachutzik, J.O., Scherzer, S., Reinders, Y., Kierszniowska, S., Schulze, W.X., Harms, G.S., Hedrich, R., Geiger, D., and Kreuzer, I. (2013). Arabidopsis nanodomain-delimited ABA signaling pathway regulates the anion channel SLAH3. Proceedings of the National Academy of Sciences of the United States of America **110**, 8296-8301.

Desvoyes, B., Ramirez-Parra, E., Xie, Q., Chua, N.H., and Gutierrez, C. (2006). Cell type-specific role of the retinoblastoma/E2F pathway during Arabidopsis leaf development. Plant physiology **140**, 67-80.

Dyson, H.J., and Wright, P.E. (2005). Intrinsically unstructured proteins and their functions. *Nature reviews. Molecular cell biology* **6**, 197-208.

Earley, K.W., Haag, J.R., Pontes, O., Opper, K., Juehne, T., Song, K., and Pikaard, C.S. (2006). Gateway-compatible vectors for plant functional genomics and proteomics. *The Plant journal : for cell and molecular biology* **45**, 616-629.

El Yahyaoui, F., Kuster, H., Ben Amor, B., Hohnjec, N., Puhler, A., Becker, A., Gouzy, J., Vernie, T., Gough, C., Niebel, A., Godiard, L., and Gamas, P. (2004). Expression profiling in *Medicago truncatula* identifies more than 750 genes differentially expressed during nodulation, including many potential regulators of the symbiotic program. *Plant physiology* **136**, 3159-3176.

Farmer, E.E., Pearce, G., and Ryan, C.A. (1989). In vitro phosphorylation of plant plasma membrane proteins in response to the proteinase inhibitor inducing factor. *Proceedings of the National Academy of Sciences of the United States of America* **86**, 1539-1542.

Fedorova, M., van de Mortel, J., Matsumoto, P.A., Cho, J., Town, C.D., VandenBosch, K.A., Gantt, J.S., and Vance, C.P. (2002). Genome-wide identification of nodule-specific transcripts in the model legume *Medicago truncatula*. *Plant physiology* **130**, 519-537.

Gietz, D., St Jean, A., Woods, R.A., and Schiestl, R.H. (1992). Improved method for high efficiency transformation of intact yeast cells. *Nucleic acids research* **20**, 1425.

Gutzat, R., Borghi, L., and Gruisse, W. (2012). Emerging roles of RETINOBLASTOMA-RELATED proteins in evolution and plant development. *Trends in plant science* **17**, 139-148.

Haney, C.H., and Long, S.R. (2010). Plant flotillins are required for infection by nitrogen-fixing bacteria. *Proceedings of the National Academy of Sciences of the United States of America* **107**, 478-483.

Haney, C.H., Riely, B.K., Tricoli, D.M., Cook, D.R., Ehrhardt, D.W., and Long, S.R. (2011). Symbiotic rhizobia bacteria trigger a change in localization and dynamics of the *Medicago truncatula* receptor kinase LYK3. *The Plant cell* **23**, 2774-2787.

Hanley-Bowdoin, L., Bejarano, E.R., Robertson, D., and Mansoor, S. (2013). Geminiviruses: masters at redirecting and reprogramming plant processes. *Nat Rev Microbiol* **11**, 777-788.

Hao, L., Wang, H., Sunter, G., and Bisaro, D.M. (2003). Geminivirus AL2 and L2 proteins interact with and inactivate SNF1 kinase. *The Plant cell* **15**, 1034-1048.

Hofgen, R., and Willmitzer, L. (1988). Storage of competent cells for Agrobacterium transformation. *Nucleic acids research* **16**, 9877.

Jacinto, T., Farmer, E.E., and Ryan, C.A. (1993). Purification of Potato Leaf Plasma Membrane Protein pp34, a Protein Phosphorylated in Response to Oligogalacturonide Signals for Defense and Development. *Plant physiology* **103**, 1393-1397.

Jarsch, I.K., and Ott, T. (2011). Perspectives on remorin proteins, membrane

rafts, and their role during plant-microbe interactions. Molecular plant-microbe interactions : MPMI **24**, 7-12.

Jarsch, I.K., Konrad, S.S., Stratil, T.F., Urbanus, S.L., Szymanski, W., Braun, P., Braun, K.H., and Ott, T. (2014). Plasma Membranes Are Subcompartmentalized into a Plethora of Coexisting and Diverse Microdomains in *Arabidopsis* and *Nicotiana benthamiana*. *The Plant cell* **26**, 1698-1711.

Jefferson, R.A., Kavanagh, T.A., and Bevan, M.W. (1987). GUS fusions: beta-glucuronidase as a sensitive and versatile gene fusion marker in higher plants. *The EMBO journal* **6**, 3901-3907.

Karimi, M., Inze, D., and Depicker, A. (2002). GATEWAY vectors for Agrobacterium-mediated plant transformation. *Trends in plant science* **7**, 193-195.

Kereszt, A., Li, D., Indrasumunhar, A., Nguyen, C.D., Nontachaiyapoom, S., Kinkema, M., and Gresshoff, P.M. (2007). Agrobacterium rhizogenes-mediated transformation of soybean to study root biology. *Nature protocols* **2**, 948-952.

Kistner, C., Winzer, T., Pitzschke, A., Mulder, L., Sato, S., Kaneko, T., Tabata, S., Sandal, N., Stougaard, J., Webb, K.J., Szczyglowski, K., and Parniske, M. (2005). Seven *Lotus japonicus* genes required for transcriptional reprogramming of the root during fungal and bacterial symbiosis. *The Plant cell* **17**, 2217-2229.

Kohn, W.D., Mant, C.T., and Hedges, R.S. (1997). Alpha-helical protein assembly motifs. *The Journal of biological chemistry* **272**, 2583-2586.

Kong, L.J., Orozco, B.M., Roe, J.L., Nagar, S., Ou, S., Feiler, H.S., Durfee, T., Miller, A.B., Gruisse, W., Robertson, D., and Hanley-Bowdoin, L. (2000). A geminivirus replication protein interacts with the retinoblastoma protein through a novel domain to determine symptoms and tissue specificity of infection in plants. *Embo Journal* **19**, 3485-3495.

Konrad, S.S., Popp, C., Stratil, T.F., Jarsch, I.K., Thallmair, V., Folgmann, J., Marin, M., and Ott, T. (2014). S-acylation anchors remorin proteins to the plasma membrane but does not primarily determine their localization in membrane microdomains. *The New phytologist*.

Kusumi, A., Fujiwara, T.K., Chadda, R., Xie, M., Tsunoyama, T.A., Kalay, Z., Kasai, R.S., and Suzuki, K.G.N. (2012). Dynamic Organizing Principles of the Plasma Membrane that Regulate Signal Transduction: Commemorating the Fortieth Anniversary of Singer and Nicolson's Fluid-Mosaic Model. *Annu Rev Cell Dev Bi* **28**, 215-250.

Lai, J., Chen, H., Teng, K., Zhao, Q., Zhang, Z., Li, Y., Liang, L., Xia, R., Wu, Y., Guo, H., and Xie, Q. (2009). RKP, a RING finger E3 ligase induced by BSCTV C4 protein, affects geminivirus infection by regulation of the plant cell cycle. *The Plant journal : for cell and molecular biology* **57**, 905-917.

Laloi, M., Perret, A.M., Chatre, L., Melser, S., Cantrel, C., Vaultier, M.N., Zachowski, A., Bathany, K., Schmitter, J.M., Vallet, M., Lessire, R., Hartmann, M.A., and Moreau, P. (2007). Insights into the role of specific lipids in the formation and delivery of lipid microdomains to the plasma membrane of plant cells. *Plant physiology* **143**, 461-472.

Latham, J.R., Saunders, K., Pinner, M.S., and Stanley, J. (1997). Induction of plant cell division by beet curly top virus gene C4. *Plant Journal* **11**, 1273-1283.

Lee, H., Hur, C.G., Oh, C.J., Kim, H.B., Pakr, S.Y., and An, C.S. (2004). Analysis of the root nodule-enhanced transcriptome in soybean. *Molecules and cells* **18**, 53-62.

Lee, S., Stenger, D.C., Bisaro, D.M., and Davis, K.R. (1994). Identification of loci in *Arabidopsis* that confer resistance to geminivirus infection. *The Plant journal : for cell and molecular biology* **6**, 525-535.

Lee, S.C., Lan, W., Buchanan, B.B., and Luan, S. (2009). A protein kinase-phosphatase pair interacts with an ion channel to regulate ABA signaling in plant guard cells. *Proceedings of the National Academy of Sciences of the United States of America* **106**, 21419-21424.

Lefebvre, B., Furt, F., Hartmann, M.A., Michaelson, L.V., Carde, J.P., Sargueil-Boiron, F., Rossignol, M., Napier, J.A., Cullimore, J., Bessoule, J.J., and Mongrand, S. (2007). Characterization of lipid rafts from *Medicago truncatula* root plasma membranes: a proteomic study reveals the presence of a raft-associated redox system. *Plant physiology* **144**, 402-418.

Lefebvre, B., Timmers, T., Mbengue, M., Moreau, S., Herve, C., Toth, K., Bittencourt-Silvestre, J., Klaus, D., Deslandes, L., Godiard, L., Murray, J.D., Udvardi, M.K., Raffaele, S., Mongrand, S., Cullimore, J., Gamas, P., Niebel, A., and Ott, T. (2010). A remorin protein interacts with symbiotic receptors and regulates bacterial infection. *Proceedings of the National Academy of Sciences of the United States*

of America **107**, 2343-2348.

Levchenko, A., Bruck, J., and Sternberg, P.W. (2000). Scaffold proteins may biphasically affect the levels of mitogen-activated protein kinase signaling and reduce its threshold properties. *Proceedings of the National Academy of Sciences of the United States of America* **97**, 5818-5823.

Lherminier, J., Elmayan, T., Fromentin, J., Elaraqui, K.T., Vesa, S., Morel, J., Verrier, J.L., Cailleteau, B., Blein, J.P., and Simon-Plas, F. (2009). NADPH oxidase-mediated reactive oxygen species production: subcellular localization and reassessment of its role in plant defense. *Molecular plant-microbe interactions : MPMI* **22**, 868-881.

Li, B., Zhang, C., Cao, B., Qin, G., Wang, W., and Tian, S. (2012a). Brassinolide enhances cold stress tolerance of fruit by regulating plasma membrane proteins and lipids. *Amino acids* **43**, 2469-2480.

Li, R., Liu, P., Wan, Y., Chen, T., Wang, Q., Mettbach, U., Baluska, F., Samaj, J., Fang, X., Lucas, W.J., and Lin, J. (2012b). A membrane microdomain-associated protein, *Arabidopsis* Flot1, is involved in a clathrin-independent endocytic pathway and is required for seedling development. *The Plant cell* **24**, 2105-2122.

Li, S., Su, X., Zhang, B., Huang, Q., Hu, Z., and Lu, M. (2013). Molecular cloning and functional analysis of the *Populus deltoides* remorin gene PdREM. *Tree physiology*.

Li, Z.Y., Li, B., and Dong, A.W. (2012c). The *Arabidopsis* transcription factor AtTCP15 regulates endoreduplication by modulating expression of key

cell-cycle genes. *Molecular plant* **5**, 270-280.

Libault, M., Farmer, A., Brechenmacher, L., Drnevich, J., Langley, R.J., Bilgin, D.D., Radwan, O., Neece, D.J., Clough, S.J., May, G.D., and Stacey, G. (2010). Complete transcriptome of the soybean root hair cell, a single-cell model, and its alteration in response to *Bradyrhizobium japonicum* infection. *Plant physiology* **152**, 541-552.

Lingwood, D., and Simons, K. (2010). Lipid Rafts As a Membrane-Organizing Principle. *Science* **327**, 46-50.

Liu, J., Elmore, J.M., Fuglsang, A.T., Palmgren, M.G., Staskawicz, B.J., and Coaker, G. (2009). RIN4 functions with plasma membrane H⁺-ATPases to regulate stomatal apertures during pathogen attack. *PLoS biology* **7**, e1000139.

Locasale, J.W., Shaw, A.S., and Chakraborty, A.K. (2007). Scaffold proteins confer diverse regulatory properties to protein kinase cascades. *Proceedings of the National Academy of Sciences of the United States of America* **104**, 13307-13312.

Lozano-Duran, R., Rosas-Diaz, T., Gusmaroli, G., Luna, A.P., Taconnat, L., Deng, X.W., and Bejarano, E.R. (2011). Geminiviruses subvert ubiquitination by altering CSN-mediated derubylation of SCF E3 ligase complexes and inhibit jasmonate signaling in *Arabidopsis thaliana*. *The Plant cell* **23**, 1014-1032.

Lu, J., Helton, T.D., Blanpied, T.A., Racz, B., Newpher, T.M., Weinberg, R.J., and Ehlers, M.D. (2007). Postsynaptic positioning of endocytic zones and AMPA receptor cycling by physical coupling of dynamin-3 to

Homer. Neuron **55**, 874-889.

Malinsky, J., Opekarova, M., Grossmann, G., and Tanner, W. (2013). Membrane microdomains, rafts, and detergent-resistant membranes in plants and fungi. Annual review of plant biology **64**, 501-529.

Marin, M., and Ott, T. (2012). Phosphorylation of intrinsically disordered regions in remorin proteins. Frontiers in plant science **3**, 86.

Marin, M., Thallmair, V., and Ott, T. (2012). The Intrinsically Disordered N-terminal Region of AtREM1.3 Remorin Protein Mediates Protein-Protein Interactions. The Journal of biological chemistry **287**, 39982-39991.

Mongrand, S., Morel, J., Laroche, J., Claverol, S., Carde, J.P., Hartmann, M.A., Bonneau, M., Simon-Plas, F., Lessire, R., and Bessoule, J.J. (2004). Lipid rafts in higher plant cells: purification and characterization of Triton X-100-insoluble microdomains from tobacco plasma membrane. The Journal of biological chemistry **279**, 36277-36286.

Muller, A., Guan, C., Galweiler, L., Tanzler, P., Huijser, P., Marchant, A., Parry, G., Bennett, M., Wisman, E., and Palme, K. (1998). AtPIN2 defines a locus of Arabidopsis for root gravitropism control. The EMBO journal **17**, 6903-6911.

Nelson, C.J., Hegeman, A.D., Harms, A.C., and Sussman, M.R. (2006). A quantitative analysis of Arabidopsis plasma membrane using trypsin-catalyzed (18)O labeling. Molecular & cellular proteomics : MCP **5**, 1382-1395.

Nohzadeh Malakshah, S., Habibi Rezaei, M., Heidari, M., and Salekdeh, G.H. (2007). Proteomics reveals new salt responsive proteins associated with rice plasma membrane. *Bioscience, biotechnology, and biochemistry* **71**, 2144-2154.

Oldroyd, G.E., Murray, J.D., Poole, P.S., and Downie, J.A. (2011). The rules of engagement in the legume-rhizobial symbiosis. *Annual review of genetics* **45**, 119-144.

Park, J., Lee, H.J., Cheon, C.I., Kim, S.H., Hur, Y.S., Auh, C.K., Im, K.H., Yun, D.J., Lee, S., and Davis, K.R. (2011). The *Arabidopsis thaliana* homeobox gene ATHB12 is involved in symptom development caused by geminivirus infection. *PloS one* **6**, e20054.

Perraki, A., Cacas, J.L., Crowet, J.M., Lins, L., Castroviejo, M., German-Retana, S., Mongrand, S., and Raffaele, S. (2012). Plasma Membrane Localization of *Solanum tuberosum* Remorin from Group 1, Homolog 3 Is Mediated by Conformational Changes in a Novel C-Terminal Anchor and Required for the Restriction of Potato Virus X Movement]. *Plant physiology* **160**, 624-637.

Perraki, A., Binaghi, M., Mecchia, M.A., Gronnier, J., German-Retana, S., Mongrand, S., Bayer, E., Zelada, A.M., and Germain, V. (2014). StRemorin1.3 hampers Potato virus X TGBp1 ability to increase plasmodesmata permeability, but does not interfere with its silencing suppressor activity. *FEBS letters*.

Raffaele, S., Bayer, E., and Mongrand, S. (2009a). Upregulation of the plant protein remorin correlates with dehiscence and cell maturation: a link with the maturation of plasmodesmata? *Plant signaling & behavior* **4**,

915-919.

Raffaele, S., Mongrand, S., Gamas, P., Niebel, A., and Ott, T. (2007). Genome-wide annotation of remorins, a plant-specific protein family: evolutionary and functional perspectives. *Plant physiology* **145**, 593-600.

Raffaele, S., Bayer, E., Lafarge, D., Cluzet, S., German Retana, S., Boubekeur, T., Leborgne-Castel, N., Carde, J.P., Lherminier, J., Noirot, E., Satiat-Jeunemaitre, B., Laroche-Traineau, J., Moreau, P., Ott, T., Maule, A.J., Reymond, P., Simon-Plas, F., Farmer, E.E., Bessoule, J.J., and Mongrand, S. (2009b). Remorin, a solanaceae protein resident in membrane rafts and plasmodesmata, impairs potato virus X movement. *The Plant cell* **21**, 1541-1555.

Rechsteiner, M., and Rogers, S.W. (1996). PEST sequences and regulation by proteolysis. *Trends in biochemical sciences* **21**, 267-271.

Reuff, M., Mikosch, M., and Homann, U. (2010). Trafficking, lateral mobility and segregation of the plant K channel KAT1. *Plant Biol (Stuttg)* **12 Suppl 1**, 99-104.

Reymond, P., Weber, H., Damond, M., and Farmer, E.E. (2000). Differential gene expression in response to mechanical wounding and insect feeding in *Arabidopsis*. *The Plant cell* **12**, 707-720.

Reymond, P., Grunberger, S., Paul, K., Muller, M., and Farmer, E.E. (1995). Oligogalacturonide defense signals in plants: large fragments interact with the plasma membrane in vitro. *Proceedings of the National Academy of Sciences of the United States of America* **92**, 4145-4149.

Reymond, P., Kunz, B., Paul-Pletzer, K., Grimm, R., Eckerskorn, C., and Farmer, E.E. (1996). Cloning of a cDNA encoding a plasma membrane-associated, uronide binding phosphoprotein with physical properties similar to viral movement proteins. *The Plant cell* **8**, 2265-2276.

Rogers, S., Wells, R., and Rechsteiner, M. (1986). Amino acid sequences common to rapidly degraded proteins: the PEST hypothesis. *Science* **234**, 364-368.

Roppolo, D., De Rybel, B., Tendon, V.D., Pfister, A., Alassimone, J., Vermeer, J.E., Yamazaki, M., Stierhof, Y.D., Beeckman, T., and Geldner, N. (2011). A novel protein family mediates Casparyan strip formation in the endodermis. *Nature* **473**, 380-383.

Shaw, A.S., and Filbert, E.L. (2009). Scaffold proteins and immune-cell signalling. *Nature reviews. Immunology* **9**, 47-56.

Shen, Q., Liu, Z., Song, F., Xie, Q., Hanley-Bowdoin, L., and Zhou, X. (2011). Tomato SlSnRK1 protein interacts with and phosphorylates betaC1, a pathogenesis protein encoded by a geminivirus beta-satellite. *Plant physiology* **157**, 1394-1406.

Shen, W., and Hanley-Bowdoin, L. (2006). Geminivirus infection up-regulates the expression of two Arabidopsis protein kinases related to yeast SNF1- and mammalian AMPK-activating kinases. *Plant physiology* **142**, 1642-1655.

Shen, W., Reyes, M.I., and Hanley-Bowdoin, L. (2009). Arabidopsis protein kinases GRIK1 and GRIK2 specifically activate SnRK1 by

phosphorylating its activation loop. *Plant physiology* **150**, 996-1005.

Shiraishi-Yamaguchi, Y., and Furuichi, T. (2007). The Homer family proteins. *Genome biology* **8**, 206.

Shiraishi, Y., Mizutani, A., Yuasa, S., Mikoshiba, K., and Furuichi, T. (2004). Differential expression of Homer family proteins in the developing mouse brain. *The Journal of comparative neurology* **473**, 582-599.

Sickmeier, M., Hamilton, J.A., LeGall, T., Vacic, V., Cortese, M.S., Tantos, A., Szabo, B., Tompa, P., Chen, J., Uversky, V.N., Obradovic, Z., and Dunker, A.K. (2007). DisProt: the Database of Disordered Proteins. *Nucleic acids research* **35**, D786-793.

Son, S. (2010). Expression pattern of soybean remorin genes and *in vitro* oligomeric status of remorin protein. M.S. thesis (Seoul National University)

Stomp, A.M. (1992). Histochemical analysis of β -glucuronidase. In GUS protocol: Using the GUS gene as a reporter of gene expression. S.R. Gallagher ed (San Diego: Academic Press Inc.) pp. 103-113

Thomas, U. (2002). Modulation of synaptic signalling complexes by Homer proteins. *J Neurochem* **81**, 407-413.

Toth, K., Stratil, T.F., Madsen, E.B., Ye, J., Popp, C., Antolin-Llovera, M., Grossmann, C., Jensen, O.N., Schussler, A., Parniske, M., and Ott, T. (2012). Functional domain analysis of the Remorin protein LjSYMREM1 in Lotus japonicus. *PloS one* **7**, e30817.

- Vanderschuren, H., Stupak, M., Futterer, J., Gruissem, W., and Zhang, P.** (2007). Engineering resistance to geminiviruses--review and perspectives. *Plant biotechnology journal* **5**, 207-220.
- Voinnet, O., Rivas, S., Mestre, P., and Baulcombe, D.** (2003). An enhanced transient expression system in plants based on suppression of gene silencing by the p19 protein of tomato bushy stunt virus. *The Plant journal : for cell and molecular biology* **33**, 949-956.
- Waadt, R., Schmidt, L.K., Lohse, M., Hashimoto, K., Bock, R., and Kudla, J.** (2008). Multicolor bimolecular fluorescence complementation reveals simultaneous formation of alternative CBL/CIPK complexes in planta. *The Plant journal : for cell and molecular biology* **56**, 505-516.
- Wang, F., Zhu, D., Huang, X., Li, S., Gong, Y., Yao, Q., Fu, X., Fan, L.M., and Deng, X.W.** (2009). Biochemical insights on degradation of Arabidopsis DELLA proteins gained from a cell-free assay system. *The Plant cell* **21**, 2378-2390.
- Wang, H., Buckley, K.J., Yang, X., Buchmann, R.C., and Bisaro, D.M.** (2005). Adenosine kinase inhibition and suppression of RNA silencing by geminivirus AL2 and L2 proteins. *Journal of virology* **79**, 7410-7418.
- Watson, B.S., Asirvatham, V.S., Wang, L., and Sumner, L.W.** (2003). Mapping the proteome of barrel medic (*Medicago truncatula*). *Plant physiology* **131**, 1104-1123.
- Widjaja, I., Naumann, K., Roth, U., Wolf, N., Mackey, D., Dangl, J.L., Scheel, D., and Lee, J.** (2009). Combining subproteome enrichment

and Rubisco depletion enables identification of low abundance proteins differentially regulated during plant defense. *Proteomics* **9**, 138-147.

Wienkoop, S., and Saalbach, G. (2003). Proteome analysis. Novel proteins identified at the peribacteroid membrane from *Lotus japonicus* root nodules. *Plant physiology* **131**, 1080-1090.

Wong, W., and Scott, J.D. (2004). AKAP signalling complexes: focal points in space and time. *Nature reviews. Molecular cell biology* **5**, 959-970.

Xiao, B., Tu, J.C., and Worley, P.F. (2000). Homer: a link between neural activity and glutamate receptor function. *Curr Opin Neurobiol* **10**, 370-374.

Yang, J.Y., Iwasaki, M., Machida, C., Machida, Y., Zhou, X., and Chua, N.H. (2008). betaC1, the pathogenicity factor of TYLCCNV, interacts with AS1 to alter leaf development and suppress selective jasmonic acid responses. *Genes & development* **22**, 2564-2577.

Zhang, X.R., Henriques, R., Lin, S.S., Niu, Q.W., and Chua, N.H. (2006). Agrobacterium-mediated transformation of *Arabidopsis thaliana* using the floral dip method. *Nature protocols* **1**, 641-646.

Zhang, Y., Immink, R., Liu, C.M., Emons, A.M., and Ketelaar, T. (2013). The *Arabidopsis* exocyst subunit SEC3A is essential for embryo development and accumulates in transient puncta at the plasma membrane. *New Phytologist* **199**, 74-88.

Zhang, Z., Chen, H., Huang, X., Xia, R., Zhao, Q., Lai, J., Teng, K., Li, Y., Liang, L., Du, Q., Zhou, X., Guo, H., and Xie, Q. (2011). BSCTV C2

attenuates the degradation of SAMDC1 to suppress DNA methylation-mediated gene silencing in *Arabidopsis*. *The Plant cell* **23**, 273-288.

Zuanazzi, J.A.S., Clergeot, P.H., Quirion, J.C., Husson, H.P., Kondorosi, A., Ratet, P. (1998). Production of *Sinorhizobium meliloti nod* gene activator and repressor flavonoids from *Medicago sativa* roots. *Mol Plant Microbe Interact* **11**, 784-794.

국문초록 (ABSTRACT IN KOREA)

식물 특이적 단백질인 리모린은 다양한 N 말단과 서로간에 보존성이 높은 C 말단으로 구성되어있으며 식물-미생물 상호작용을 포함한 다양한 스트레스 반응에 관련되어 있을 것으로 예상된다. 하지만 리모린의 기능에 대하여서는 아직 정확히 알려져 있지 않으며 특히 애기장대 리모린 4 그룹 및 콩 리모린에 대하여서는 전혀 연구가 되어 있지 않다. 따라서 본 연구에서는 콩의 뿌리혹 발달과정에서 발현이 증가하는 리모린과 애기장대 4그룹에 속하는 리모린의 기능에 대하여 분석하였다.

1장에서는 콩의 뿌리혹 발달과정에서 발현이 증가하는 두 유전자인 *GmREM1.1*과 *GmREM2.1*의 분자적 특성 및 기능적 차이에 대하여 연구하였다. *GmREM1.1* 단백질의 CA 부위는 세포막 이동에 필수적이었지만, *GmREM2.1* 단백질의 CA 부위는 세포막으로 이동하지 못했다. 그리고 *GmREM1.1/1.3*은 서로 상호결합하여 중합체를 형성하였지만 *GmREM2.1*과는 결합하지 않았다. 또한

형질전환 된 콩의 뿌리혹에서 *GmREM1.1*의 프로모터는 내피질에서 활성화 되었지만 *GmREM2.1*의 프로모터는 감염세포에서 활성화 되었고, *GmREM2.1*의 경우 발현이 억제되면 뿌리혹의 개수가 줄어들었지만 *GmREM1.1*의 경우는 발현이 억제되어도 뿌리혹 형성에는 큰 차이가 없었다. 이러한 결과들을 통하여 *GmREM1.1*과 *GmREM2.1*이 서로 다른 분자적 특성을 가지며 뿌리혹 형성과정에서 서로 다른 기능을 수행함을 제시하였다.

2장에서는 리모린 4그룹에 속하는 애기장대 유전자인 *AtREM4.1*과 *AtREM4.2*의 생물학적 기능에 대하여 연구하였다. *AtREM4s*는 다양한 삼투, ABA 및 노화에 의해 발현이 현격하게 증가하며 세포막 위치 및 중합체형성과 같은 전형적인 리모린의 분자적 특성을 가지고 있었다. 제미니바이러스 감염 시 두 유전자의 이중돌연변이체에서는 감염증상이 현격히 억제되었지만 과발현체들에서는 감염이 오히려 증가하였다. *AtREM4* 단백질들은 SnRK1 및 26S proteasome에 의하여 조절 되었으며, *AtREM4.1*은 전사 인자인 AtTCP14와 결합하여 핵으로 이동하였다. 이러한 결과들을 토대로, 애기장대 4그룹 리모린은 제미니바이러스 감염 시 SnRK1-AtTCP14 신호전달과정에 관여하여 세포분열을 조절하는 역할을 수행할 것으로 예상된다.

주요어: 애기장대 리모린, 제미니바이러스, 콩 리모린, 뿌리혹,

SNF1-연관 인산화효소 1

학번: 2010-30098